Achieving a Continuous Diversity-Complexity Tradeoff in Wireless MIMO Systems via Pre-Equalized Sphere-Decoding

Johannes Maurer, *Student Member, IEEE*, Joakim Jaldén, *Member, IEEE*, Dominik Seethaler, *Member, IEEE*, and Gerald Matz, *Senior Member, IEEE*

***Abstract*—In multiple-input multiple-output (MIMO) spatial multiplexing systems, maximum-likelihood (ML) detection achieves maximum diversity at the cost of high computational complexity. In contrast, low-complexity alternatives like zero-forcing (ZF) detection suffer from a significant diversity loss. In this paper, we present a novel detection scheme that allows a continuous tradeoff between diversity order and complexity reduction. The proposed detector consists of two stages: the first stage is a linear pre-equalizer that partially eliminates MIMO interference and improves the channel condition number; the second stage is a mismatched ML detector on the residual channel that ignores the correlation introduced by the equalization stage. This second stage is implemented using a variant of the sphere decoder. ML and ZF detection are extreme special cases of our novel scheme. We give insights into the main effects that determine performance and we provide an explicit expression for the diversity order achieved with the proposed detector. Simulation results confirm that our scheme allows to trade diversity for complexity savings in a continuous manner.**

***Index Terms*—Condition number, diversity, large deviation principle, maximum-likelihood (ML) detection, multiple-input multiple-output (MIMO) spatial multiplexing, sphere decoding, zero-forcing detection.**

I. Introduction

TWO OF THE most important benefits of multiple-input multiple-output (MIMO) wireless systems are increased capacity (multiplexing gain) and improved reliability (diversity gain) [1]. In this paper, we consider spatial multiplexing systems with M_{T} transmit antennas and M_{R} receive antennas. Such systems offer a multiplexing gain of M_{T} and allow for a receive diversity gain of $d_{\max} = M_{\mathrm{R}}$, provided that appropriate detection algorithms are used. The optimum detector providing full diversity is the maximum-likelihood (ML) detector. Unfortunately, ML detection is computationally very expensive. Even the sphere decoder implementation [2], [3] of the ML detector has a worst-case and average complexity that grows exponentially with the number of transmit antennas M_{T} under independent and identically distributed (i.i.d.) Rayleigh fading [4], [5]. At the opposite extreme are low-complexity suboptimum detection schemes like zero-forcing (ZF), minimum mean squared error (MMSE), decision-feedback detection [6]–[8], all of which only achieve a diversity order of $d_{\min} = M_{\mathrm{R}} - M_{\mathrm{T}} + 1$. This can be attributed to the fact that sub-optimum detectors perform poorly for channels with large condition number [9], [10]. However, when preceded by LLL lattice reduction (LR) [11], sub-optimum detectors retain full diversity [12]. The sub-optimum fixed-complexity sphere decoder [13] achieves full diversity order $d_{\max}$ with fixed (i.e., channel-independent) complexity. It is interesting to observe that most MIMO detection schemes in the literature achieve either full diversity order $d_{\max}$ or the poor diversity order $d_{\min}$, with a few exceptions (e.g., [7], [14]) that achieve integer diversity order in between these two extremes. However, none of the detection schemes proposed so far allows arbitrary (non-integer) diversity orders between $d_{\min}$ and $d_{\max}$ in a scalable manner.

In this paper, we propose a novel MIMO detector that allows to trade diversity and complexity in a continuous manner and comprises ML and ZF detection as special cases. Our scheme consists of two stages. The first stage partially equalizes the channel, resulting in a channel with a smaller condition number. The second stage performs *mismatched* ML detection in the sense that the noise correlation introduced by the first stage is ignored. This second stage is implemented via a sphere decoder variant [15] that is suited for low signal-to-noise ratios (SNRs). The overall scheme will henceforth be referred to as *pre-equalized sphere decoding (PSD)* detection. The diversity and complexity of the scheme essentially depend on the amount of equalization, which is controlled by a scalar parameter α. We use large deviation arguments [16] to identify the dominant error events for our proposed scheme and thereby analytically derive its diversity order as a function of α. We also analyze the overall complexity of the proposed detector and show that the equalization parameter α allows to control the complexity of the sphere decoder in the second stage.

This paper is organized as follows. In Section II, we describe the system model and reformulate ML and ZF detection in a unified framework. PSD is introduced in Section III and an efficient sphere decoder implementation is developed in Section IV. In

Manuscript received September 01, 2008; revised August 29, 2009. Current version published January 13, 2010. This work was supported by the STREP project MASCOT (IST-026905) within the Sixth Framework Program of the European Commission. The associate editor coordinating the review of this manuscript and approving it for publication was Dr. Robert Calderbank.

J. Maurer, J. Jaldén, and G. Matz are with the Institute of Communications and Radio-Frequency Engineering, Vienna University of Technology, 1040 Vienna, Austria (e-mail: jmaurer@nt.tuwien.ac.at; jjalden@nt.tuwien.ac.at; gmatz@nt.tuwien.ac.at).

D. Seethaler is with the Communication Technology Lab, ETH Zurich, CH-8092 Zurich, Switzerland (e-mail: seethal@nari.ee.ethz.ch).

Color versions of one or more of the figures in this paper are available online at http://ieeexplore.ieee.org.

Digital Object Identifier 10.1109/JSTSP.2009.2038210

Section V, we derive the diversity order of PSD. Simulation results are presented in Section VI and conclusions are provided in Section VII. Detailed derivations and proofs are relegated to the Appendices.

II. System Model and Classical Detectors

A. System Model

We assume a linear MIMO spatial multiplexing system where $M_{\mathrm{R}} \geq M_{\mathrm{T}}$. The entries of the transmit vector $\mathbf{x} \in \mathcal{A}^{M_{\mathrm{T}}}$ (with $\mathcal{A}$ denoting the symbol alphabet) are i.i.d. with $\mathrm{E}\{\mathbf{x}\mathbf{x}^H\} = \mathbf{I}$. Assuming a flat-fading channel, the length-M_{R} receive vector equals

$$\mathbf{r} = \mathbf{H}\mathbf{x} + \mathbf{n}. \tag{1}$$

Here, $\mathbf{H}$ is the $M_{\mathrm{R}} \times M_{\mathrm{T}}$ channel matrix (assumed perfectly known at the receiver), whose elements $[\mathbf{H}]_{n,m}$ are the complex fading coefficients between the mth transmit antenna and the nth receive antenna. Furthermore, $\mathbf{n} \sim \mathcal{CN}(\mathbf{0}, \sigma_n^2\mathbf{I})$ denotes spatially white complex Gaussian noise with variance σ_n^2. The signal-to-noise ratio (SNR) at the receiver is defined as $\mathrm{SNR} = \mathrm{E}\left\{\|\mathbf{H}\mathbf{x}\|^2\right\}/\mathrm{E}\left\{\|\mathbf{n}\|^2\right\}$.

B. ML Detection

With our assumption of i.i.d. Gaussian noise, ML detection amounts to solving [1]–[3]

$$\hat{\mathbf{x}}_{\mathrm{ML}} = \underset{\mathbf{x}\in\mathcal{A}^{M_{\mathrm{T}}}}{\arg\min} \|\mathbf{r} - \mathbf{H}\mathbf{x}\|^2$$

which achieves the minimum vector error probability for uniformly distributed transmit vectors. Even when implemented using the sphere-decoding algorithm [2], [3] the computational complexity of ML detection in general grows exponentially with M_{T} [4].

For a given channel realization $\mathbf{H}$, the pairwise error probability (PEP) of ML detection, i.e., the probability that the detector prefers $\mathbf{x}_2$ over $\mathbf{x}_1$ when $\mathbf{x}_1$ was actually transmitted, equals [1]

$$P(\mathbf{x}_1 \rightarrow \mathbf{x}_2|\mathbf{H}) = \mathrm{Q}\left(\frac{\|\mathbf{H}\boldsymbol{\delta}\|}{\sqrt{2}\sigma_n}\right). \tag{2}$$

Here, $\boldsymbol{\delta} = \mathbf{x}_1 - \mathbf{x}_2$ is the error vector and $\mathrm{Q}(\cdot)$ denotes the Q-function. For i.i.d. Rayleigh fading, the mean PEP for ML detection is upper bounded as [1]

$$\begin{aligned} P(\mathbf{x}_1 \rightarrow \mathbf{x}_2) &= \mathrm{E}_{\mathbf{H}}\{P(\mathbf{x}_1 \rightarrow \mathbf{x}_2|\mathbf{H})\} \\ &\leq C_{\mathrm{ML}} \left(1 + \frac{\|\boldsymbol{\delta}\|^2}{4\sigma_n^2}\right)^{-M_{\mathrm{R}}} \end{aligned} \tag{3}$$

where C_{ML} is a positive constant. We define the diversity order achieved by a detector as

$$d = \lim_{\sigma_n^2 \to 0} \frac{\log P(\mathbf{x}_1 \rightarrow \mathbf{x}_2)}{\log \sigma_n^2}. \tag{4}$$

It follows from (3) that for ML detection $d = M_{\mathrm{R}} = d_{\max}$, i.e., the ML detector achieves full diversity (at the expense of a computational complexity that is exponential in M_{T}).

C. ZF Detection

With ZF equalization, the receive vector is first passed through a channel equalizer that cancels MIMO interference, i.e.,

$$\mathbf{y} = \mathbf{H}^{\#}\mathbf{r} = \mathbf{x} + \mathbf{H}^{\#}\mathbf{n} \tag{5}$$

where $\mathbf{H}^{\#} = (\mathbf{H}^H\mathbf{H})^{-1}\mathbf{H}^H$ denotes the pseudo-inverse of $\mathbf{H}$ [17]. The ZF-equalized vector $\mathbf{y}$ is then fed to a slicer that yields the detected transmit vector

$$\hat{\mathbf{x}}_{\mathrm{ZF}} = \mathcal{Q}_{\mathcal{A}}\{\mathbf{y}\}. \tag{6}$$

Here, $\mathcal{Q}_{\mathcal{A}}\{\cdot\}$ denotes element-wise quantization with respect to the symbol alphabet $\mathcal{A}$.

For a given $\mathbf{H}$, the PEP of the ZF detector can be written as [18]

$$P(\mathbf{x}_1 \rightarrow \mathbf{x}_2|\mathbf{H}) = \mathrm{Q}\left(\frac{1}{\sqrt{2}\sigma_n}\frac{\|\boldsymbol{\delta}\|^2}{\sqrt{\boldsymbol{\delta}^H(\mathbf{H}^H\mathbf{H})^{-1}\boldsymbol{\delta}}}\right)$$

and for i.i.d. Rayleigh fading the mean PEP is bounded as [19]

$$P(\mathbf{x}_1 \rightarrow \mathbf{x}_2) \leq C_{\mathrm{ZF}} \left(1 + \frac{\|\boldsymbol{\delta}\|^2}{4\sigma_n^2}\right)^{-M_{\mathrm{R}}+M_{\mathrm{T}}-1}$$

where C_{ZF} is a positive constant. The ZF detector thus yields a diversity order of $d_{\mathrm{ZF}} = M_{\mathrm{R}} - M_{\mathrm{T}} + 1 = d_{\min}$ with the advantage of requiring low computational effort.

D. Unified Framework for ML and ZF Detection

In order to place ML and ZF detection on a common basis, we reconsider the ZF domain relation $\mathbf{y} = \mathbf{x} + \mathbf{H}^{\#}\mathbf{n}$ [cf. (5)]. The noise $\mathbf{H}^{\#}\mathbf{n}$ after ZF equalization is distributed as $\mathbf{H}^{\#}\mathbf{n} \sim \mathcal{CN}(\mathbf{0}, \sigma_n^2\mathbf{G}^{-1})$, where $\mathbf{G} = \mathbf{H}^H\mathbf{H}$ denotes the Gram matrix of $\mathbf{H}$. Hence, the ZF equalizer in general renders the components of $\mathbf{H}^{\#}\mathbf{n}$ correlated.

The ZF domain receive vector $\mathbf{y}$ is a sufficient statistic for detecting $\mathbf{x}$ and has conditional distribution $\mathbf{y}|\mathbf{x} \sim \mathcal{CN}(\mathbf{x}, \sigma_n^2\mathbf{G}^{-1})$. In fact, the ML detector (2) can be straightforwardly rewritten as

$$\hat{\mathbf{x}}_{\mathrm{ML}} = \underset{\mathbf{x}\in\mathcal{A}^{M_{\mathrm{T}}}}{\arg\min} (\mathbf{y} - \mathbf{x})^H\mathbf{G}(\mathbf{y} - \mathbf{x}). \tag{7}$$

In contrast, ZF detection ignores the noise correlation in the ZF domain. The component-wise quantization (6) performed by the ZF detector can be reformulated as

$$\hat{\mathbf{x}}_{\mathrm{ZF}} = \underset{\mathbf{x}\in\mathcal{A}^{M_{\mathrm{T}}}}{\arg\min} (\mathbf{y} - \mathbf{x})^H(\mathbf{y} - \mathbf{x}). \tag{8}$$

Both ML and ZF detection can thus be written in terms of a positive definite quadratic form in the error vector $\mathbf{y} - \mathbf{x}$, the difference being that with ML detection the quadratic form is induced by $\mathbf{G} = \mathbf{G}^1$ whereas with ZF detection it is induced by $\mathbf{I} = \mathbf{G}^0$. The ML detector thus fully exploits the noise correlation in the ZF domain, whereas the ZF detector ignores the noise correlation completely.

III. Pre-Equalized Sphere Decoding

A. Mismatched ML Metric

The unified formulation of ML and ZF detection in the previous subsection motivates us to propose a class of receivers which use a similar detection metric as (7) and (8) but with arbitrary powers (between 0 and 1) of the Gram matrix, i.e.,

$$\hat{\mathbf{x}}_\alpha = \underset{\mathbf{x}\in\mathcal{A}^{M_\mathrm{T}}}{\arg\min} (\mathbf{y}-\mathbf{x})^H \mathbf{G}^{1-\alpha}(\mathbf{y}-\mathbf{x}), \quad 0 \le \alpha \le 1. \tag{9}$$

Here, $\mathbf{G}^{1-\alpha} = \sum_{k=1}^{M_\mathrm{T}} \lambda_k^{1-\alpha}\, \mathbf{v}_k\, \mathbf{v}_k^H$, with $\lambda_k > 0$, and $\mathbf{v}_k$, respectively, denoting the (necessarily real and positive) eigenvalues and (normalized) eigenvectors of the Gram matrix [17]. The metric in (9) can be interpreted as ML metric for the model $\mathbf{y} = \mathbf{x} + \mathbf{w}$ under the assumption that the noise has distribution $\mathbf{w} \sim \mathcal{CN}(\mathbf{0}, \sigma_n^2 \mathbf{G}^{\alpha-1})$. However, the actual noise in the ZF domain is distributed as $\mathbf{H}^{\#}\mathbf{n} \sim \mathcal{CN}(\mathbf{0}, \sigma_n^2 \mathbf{G}^{-1})$. Since for $\alpha \neq 0$ the true noise correlation is only partially taken into account, the metric in (9) is not matched to the actual system model and hence amounts to a *mismatched ML detector*.

The set of symbol estimates defined by (9) provides a means to move continuously from the ML solution $\hat{\mathbf{x}}_0 = \hat{\mathbf{x}}_\mathrm{ML}$ to the ZF solution $\hat{\mathbf{x}}_1 = \hat{\mathbf{x}}_\mathrm{ZF}$. This suggests that the performance and complexity of (9) will scale with α, thereby providing a tradeoff between ML and ZF detection. The rest of this paper is dedicated to showing that this tradeoff in fact exists. Since the distance $\sigma_n^2 \|\mathbf{G}^{\alpha-1} - \mathbf{G}^{-1}\|_\mathrm{F}$ between the mismatched correlation $\sigma_n^2 \mathbf{G}^{\alpha-1}$ and the true correlation $\sigma_n^2 \mathbf{G}^{-1}$ can be shown to be a monotonically increasing function of α, it is quite plausible that the performance of the mismatched ML detector (9) will decrease with increasing α. A precise formulation and proof of this statement in terms of receive diversity is provided in Section V. On the other hand, it is not so obvious that (9) enables more and more complexity savings with increasing α. Before providing a detailed discussion of an implementation for which this is indeed the case, we give a short heuristic argument.

It is known [2], [3], [9] that the complexity of ML detection using sphere decoding depends crucially on the channel condition number (i.e., the ratio of the largest and smallest singular value [17]). Since (9) amounts to an ML detection problem (even though a mismatched one), the condition number $\kappa(\mathbf{G}^{1-\alpha})$ of the matrix $\mathbf{G}^{1-\alpha}$ influences the complexity of (9). Straightforward linear algebra implies that $\kappa(\mathbf{G}^{1-\alpha}) = \kappa^{1-\alpha}(\mathbf{G})$, i.e., the condition number of $\mathbf{G}^{1-\alpha}$ decays exponentially with α. For $0 \le \alpha_1 \le \alpha_2 \le 1$, we have

$$\kappa(\mathbf{G}) \ge \kappa(\mathbf{G}^{1-\alpha_1}) \ge \kappa(\mathbf{G}^{1-\alpha_2}) \ge 1,$$

suggesting that the complexity of (9) decreases with increasing α.

A generalized version of the mismatched ML detector (9), not further considered in this paper, is obtained by using an arbitrary positive definite matrix $\mathbf{F}$ to induce a quadratic form in the ZF domain

$$\hat{\mathbf{x}} = \underset{\mathbf{x}\in\mathcal{A}^{M_\mathrm{T}}}{\arg\min} (\mathbf{y}-\mathbf{x})^H \mathbf{F}(\mathbf{y}-\mathbf{x}). \tag{10}$$

The choice of the matrix $\mathbf{F}$ again determines the performance and complexity of (10). For example, choosing $\mathbf{F}$ as a block diagonal matrix approximating $\mathbf{G}$ admits a reduced-complexity sphere decoder implementation at the expense of a certain performance degradation (cf. [20] for such an approach applied to code division multiple access systems).

B. Two-Stage Reformulation

We next derive a two-stage implementation of the ZF domain problem (9) which applies directly to the receive vector $\mathbf{r}$ and is more convenient for implementation and interpretation. To this end, we rewrite the quadratic form in (9) as

$$\begin{aligned}(\mathbf{y}-\mathbf{x})^H \mathbf{G}^{1-\alpha}(\mathbf{y}-\mathbf{x}) &= (\mathbf{y}-\mathbf{x})^H \left[\mathbf{G}^{(1-\alpha)/2}\right]^H \mathbf{G}^{(1-\alpha)/2}(\mathbf{y}-\mathbf{x}) \\ &= \left\|\mathbf{G}^{(1-\alpha)/2}\mathbf{y} - \mathbf{G}^{(1-\alpha)/2}\mathbf{x}\right\|^2. \end{aligned} \tag{11}$$

where $\mathbf{G}^{(1-\alpha)/2} = \mathbf{V}\mathbf{\Lambda}^{(1-\alpha)/2}\mathbf{V}^H$ denotes the positive definite square-root of $\mathbf{G}^{1-\alpha}$ (here, $\mathbf{V} = (\mathbf{v}_1 \cdots \mathbf{v}_{M_\mathrm{T}})$ and $\mathbf{\Lambda} = \mathrm{diag}\{\lambda_k\}_{k=1}^{M_\mathrm{T}}$). To further simplify this expression, we use the SVD $\mathbf{H} = \mathbf{U}\mathbf{D}\mathbf{V}^H$ of the channel matrix. We denote the first term on the right-hand side in (11) as $\tilde{\mathbf{r}}_\alpha = \mathbf{G}^{(1-\alpha)/2}\mathbf{y}$ and develop it as follows:

$$\begin{aligned}\tilde{\mathbf{r}}_\alpha &= \mathbf{G}^{(1-\alpha)/2}\mathbf{y} = \mathbf{G}^{(1-\alpha)/2}\mathbf{H}^{\#}\mathbf{r} \\ &= \mathbf{V}\mathbf{\Lambda}^{(1-\alpha)/2}\mathbf{V}^H\mathbf{V}\mathbf{D}^{-1}\mathbf{U}^H\mathbf{r} \\ &= \mathbf{V}\mathbf{D}^{-\alpha}\mathbf{U}^H\mathbf{r} = \mathbf{W}_\alpha^{-1}\mathbf{r} \end{aligned} \tag{12}$$

where we used that $\mathbf{H}^{\#} = \mathbf{V}\mathbf{D}^{-1}\mathbf{U}^H$, $\mathbf{V}$ is unitary, and $\mathbf{\Lambda} = \mathbf{D}^2$. Hence, $\tilde{\mathbf{r}}_\alpha$ amounts to applying a *partial equalizer* $\mathbf{W}_\alpha^{-1} = \mathbf{V}\mathbf{D}^{-\alpha}\mathbf{U}^H$ to the receive vector $\mathbf{r}$ (observe that for $\alpha = 1$ the ZF equalizer is obtained, i.e., $\mathbf{W}_1^{-1} = \mathbf{H}^{\#}$). Inserting (1) into (12) yields

$$\tilde{\mathbf{r}}_\alpha = \mathbf{W}_\alpha^{-1}(\mathbf{H}\mathbf{x} + \mathbf{n}) = \mathbf{C}_\alpha \mathbf{x} + \tilde{\mathbf{n}}_\alpha \tag{13}$$

where $\tilde{\mathbf{n}}_\alpha = \mathbf{W}_\alpha^{-1}\mathbf{n} \sim \mathcal{CN}(\mathbf{0}, \sigma_n^2 \mathbf{G}^{-\alpha})$ denotes spatially correlated noise and $\mathbf{C}_\alpha = \mathbf{W}_\alpha^{-1}\mathbf{H}$ denotes the residual part of the channel that remains unequalized. It turns out that

$$\mathbf{C}_\alpha = \mathbf{V}\mathbf{D}^{-\alpha}\mathbf{U}^H\mathbf{U}\mathbf{D}\mathbf{V}^H = \mathbf{V}\mathbf{D}^{1-\alpha}\mathbf{V}^H = \mathbf{G}^{(1-\alpha)/2} \tag{14}$$

which finally allows us to rewrite (9) as

$$\hat{\mathbf{x}}_\alpha = \underset{\mathbf{x}\in\mathcal{A}^{M_\mathrm{T}}}{\arg\min} \left\|\tilde{\mathbf{r}}_\alpha - \mathbf{C}_\alpha \mathbf{x}\right\|^2. \tag{15}$$

This expression looks like the ML detector for the linear model (13) apart from the fact that the correlation $\sigma_n^2 \mathbf{G}^{-\alpha}$ of the noise $\tilde{\mathbf{n}}_\alpha$ is being ignored. Clearly, the mismatched ML detector (9) is reformulated in terms of a squared distance in a pre-equalized domain instead of a quadratic form in the ZF domain. Taken together, (12) and (15) show that the scheme proposed in (9) can be implemented in terms of two stages (cf. Fig. 1): the first stage pre-equalizes the channel and the second stage performs mismatched ML detection by ignoring the noise correlation introduced by the partial equalizer.

The parameter α can now be interpreted as the amount of pre-equalization. For $\alpha = 0$, there is no pre-equalization; in this

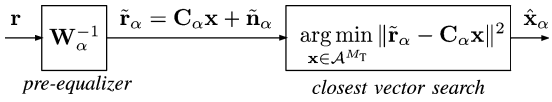

Fig. 1. Block diagram of proposed detector consisting of a pre-equalizer followed by a closest vector search.

case, $\mathbf{W}_0^{-1}$ amounts to a distance-preserving unitary rotation and there is actually no mismatch in the second stage, i.e.,

$$\begin{aligned}\hat{\mathbf{x}}_0 &= \arg\min_{\mathbf{x}\in\mathcal{A}^{M_\mathrm{T}}} \left\|\tilde{\mathbf{r}}_0 - \mathbf{C}_0\mathbf{x}\right\|^2 \\ &= \arg\min_{\mathbf{x}\in\mathcal{A}^{M_\mathrm{T}}} \left\|\mathbf{r} - \mathbf{H}\mathbf{x}\right\|^2 = \hat{\mathbf{x}}_\mathrm{ML}.\end{aligned}$$

On the other hand, for $\alpha = 1$ there is $\mathbf{W}_1^{-1} = \mathbf{H}^{\#}$ and $\mathbf{C}_1 = \mathbf{I}$, i.e., the channel is fully equalized and $\hat{\mathbf{x}}_1 = \arg\min_{\mathbf{x}\in\mathcal{A}^{M_\mathrm{T}}} \left\|\mathbf{H}^{\#}\mathbf{r} - \mathbf{x}\right\|^2 = \mathcal{Q}_\mathcal{A}\left\{\mathbf{H}^{\#}\mathbf{r}\right\} = \hat{\mathbf{x}}_\mathrm{ZF}$ leads to the ZF solution. Generally speaking, for small α there is little equalization and correspondingly almost no noise correlation is ignored in the second stage, whereas for large α the mismatched ML detector ignores potentially strong noise correlation; however, in this case the channel is almost fully equalized, which can be exploited to reduce complexity.

IV. Sphere Decoder Implementation

In this section, we use a variant of the sphere decoder (SD) to provide an implementation of our proposed detector whose complexity decreases continuously with α. Before doing so, we argue that the classical SD is not able to provide the desired behavior.

A. Conventional SD

We first provide a very brief review of how the SD solves the closest vector problem (15) in an efficient manner [2]. The fundamental idea of SD is to limit the search to a subset of vectors that lie within a sphere of radius R around the receive vector (in our case $\tilde{\mathbf{r}}_\alpha$). Using the QR decomposition $\mathbf{C}_\alpha = \mathbf{Q}\mathbf{R}$ [21] to transform the residual channel into upper triangular form, the metric in (15) can be rewritten as [22]

$$\left\|\tilde{\mathbf{r}}_\alpha - \mathbf{C}_\alpha\mathbf{x}\right\|^2 = \left\|\mathbf{q} - \mathbf{R}\mathbf{x}\right\|^2 \tag{16}$$

where $\mathbf{q} = \mathbf{Q}^H\tilde{\mathbf{r}}_\alpha$. Searching for the solution within the hypersphere $\left\|\mathbf{q} - \mathbf{R}\mathbf{x}\right\|^2 \le R^2$ amounts to a branch-and-bound-like traversal of a regular tree with M_T layers and $|\mathcal{A}|$ children per node (each node corresponding to a partial transmit vector). Specifically, $\mathbf{R}$, $\mathbf{q}$ and $\mathbf{x}$ are partitioned according to

$$\mathbf{R} = \begin{bmatrix}\mathbf{R}_k^{(11)} & \mathbf{R}_k^{(12)} \\ \mathbf{0} & \mathbf{R}_k^{(22)}\end{bmatrix} \quad \mathbf{q} = \begin{bmatrix}\mathbf{q}_k^{(1)} \\ \mathbf{q}_k^{(2)}\end{bmatrix} \quad \text{and} \quad \mathbf{x} = \begin{bmatrix}\mathbf{x}_k^{(1)} \\ \mathbf{x}_k^{(2)}\end{bmatrix}$$

where the blocks $\mathbf{R}_k^{(11)}$, $\mathbf{R}_k^{(12)}$, and $\mathbf{R}_k^{(22)}$ have respective dimension $(M_\mathrm{T}-k)\times(M_\mathrm{T}-k)$, $(M_\mathrm{T}-k)\times k$, and $k\times k$; furthermore, $\mathbf{q}_k^{(1)}$ and $\mathbf{q}_k^{(2)}$ correspond to the first $M_\mathrm{T}-k$ and last k elements of $\mathbf{q}$, respectively, and $\mathbf{x}_k^{(1)}$ and $\mathbf{x}_k^{(2)}$ are defined similarly. The metric (16) can then also be split into two terms corresponding to the first $M_\mathrm{T}-k$ and the last k layers

$$\begin{aligned}\left\|\mathbf{q} - \mathbf{R}\mathbf{x}\right\|^2 = &\left\|\mathbf{q}_k^{(1)} - \mathbf{R}_k^{(11)}\mathbf{x}_k^{(1)} - \mathbf{R}_k^{(12)}\mathbf{x}_k^{(2)}\right\|^2 \\ &+\left\|\mathbf{q}_k^{(2)} - \mathbf{R}_k^{(22)}\mathbf{x}_k^{(2)}\right\|^2.\end{aligned} \tag{17}$$

According to (17), a necessary condition for $\left\|\mathbf{q} - \mathbf{R}\mathbf{x}\right\|^2 \le R^2$ that involves only already visited nodes is given by

$$\left\|\mathbf{q}_k^{(2)} - \mathbf{R}_k^{(22)}\mathbf{x}_k^{(2)}\right\|^2 \le R^2. \tag{18}$$

Hence, all transmit vectors whose last k elements violate (18) can be discarded from the tree search since they cannot satisfy the sphere constraint $\left\|\mathbf{q} - \mathbf{R}\mathbf{x}\right\|^2 \le R^2$. The sphere decoder repeatedly applies (18) for $k = 1, \ldots, M_\mathrm{T}$ to prune the set of candidate solutions. There is now a large body of literature that discusses the efficient implementation of this procedure, and also how to choose and update the search radius R, see, e.g., [2], and [23]–[25]. However, the SD complexity grows exponentially in M_T, no matter how the radius is updated [5]. In the following, we will use the Schnorr–Euchner SD strategy [2], [26] (in the complex domain), which does not require that the search radius is selected prior to the search.

B. Impact of α on SD Complexity

The complexity of SD in terms of the number of nodes visited depends on the channel matrix $\mathbf{C}_\alpha$, the transmit vector $\mathbf{x}$, and the noise $\tilde{\mathbf{n}}_\alpha$. It seems difficult to provide a closed-form expression for the complexity of SD based on the Schnorr–Euchner enumeration strategy. Hence, we resort to the condition number of the channel (cf. [24], [27]) and the effective SNR [22] as simple heuristics influencing, the SD's computational complexity.

1) Condition Number: If $\mathbf{C}_\alpha$ (and thus $\mathbf{R}$) has a small condition number, this tends to reduce the SD complexity [24], [27]. The rationale here is that if $\mathbf{R}$ is poorly conditioned, the elements of $\mathbf{R}_k^{(22)}$ for k close to M_T tend to be small and hence (18) does not allow for aggressive tree pruning. Clearly, (14) implies that

$$\kappa(\mathbf{C}_\alpha) = \kappa\big(\mathbf{G}^{(1-\alpha)/2}\big) = \kappa^{(1-\alpha)/2}(\mathbf{G}) = \kappa^{1-\alpha}(\mathbf{H}).$$

Thus, the condition number of $\mathbf{C}_\alpha$ is a strictly monotonically decreasing function of α (unless $\kappa(\mathbf{H}) = 1$, in which case it is constant). For the extreme case $\alpha = 1$ we have $\kappa(\mathbf{C}_1) = 1$ which implies that $\mathbf{C}_1$ is unitary (in fact, $\mathbf{C}_1 = \mathbf{I}$).

2) Effective SNR: Large effective SNR, i.e., small total noise power $\|\tilde{\mathbf{n}}_\alpha\|^2$ generally allows for a small sphere radius R (note that $\|\mathbf{q} - \mathbf{R}\mathbf{x}\|^2 = \|\tilde{\mathbf{n}}_\alpha\|^2$ if $\mathbf{x}$ is the actual transmit vector), which in turn allows for more aggressive tree pruning via (18). Hence, SD complexity benefits greatly from increased SNR (cf.

[22]). The instantaneous SNR in the equivalent model (13) is given by

$$\mathrm{snr}_\alpha = \frac{\mathrm{E}\{\|\mathbf{C}_\alpha \mathbf{x}\|^2 | \mathbf{C}_\alpha\}}{\mathrm{E}\{\|\tilde{\mathbf{n}}_\alpha\|^2 | \mathbf{C}_\alpha\}}. \tag{19}$$

It is shown in Appendix A that snr_α is a strictly decreasing function in α (unless $\kappa(\mathbf{H}) = 1$, in which case it is constant). Hence, with increasing α the pre-equalizer causes increasing noise enhancement, the worst case being ZF equalization ($\alpha = 1$).

Increasing α improves the condition number but simultaneously deteriorates the effective SNR and it is not clear which effect will dominate. Since conventional SD requires high SNR to yield low complexity, it is therefore not granted that increasing α here will necessarily lead to complexity reduction. Fortunately, the low SNR behavior of the SD has been previously investigated and improved sphere decoders, which are less sensitive to SNR, have been proposed in the literature.

C. SD Variant

To exploit the improved condition number for large α in spite of strong noise enhancement, we propose to use a SD variant which has been introduced in [15] and which is well suited for the low-SNR regime. The main idea is to improve the tree pruning by using a tighter sphere bound than (18), which was obtained by observing that the first term on the right-hand side of (17) is non-negative. However, this first term can be more tightly bounded using the Rayleigh–Ritz theorem [17], as shown in (20) at the bottom of the page, where $\sigma^2_{\min}\big(\mathbf{R}_k^{(11)}\big)$ denotes the smallest singular value of $\mathbf{R}_k^{(11)}$ and $\mathbf{b}_k = \big(\mathbf{R}_k^{(11)}\big)^{-1}\big(\mathbf{q}_k^{(1)} - \mathbf{R}_k^{(12)}\mathbf{x}_k^{(2)}\big)$. Even though $\mathbf{x}_k^{(1)}$ is unknown at layer k, the fact that $\mathbf{x}_k^{(1)} \in \mathcal{A}^{M_\mathrm{T}-k}$ implies $\big\|\mathbf{b}_k - \mathbf{x}_k^{(1)}\big\|^2 \geq \|\mathbf{b}_k - \mathcal{Q}_\mathcal{A}\{\mathbf{b}_k\}\|^2$, where $\mathcal{Q}_\mathcal{A}\{\cdot\}$ denotes element-wise quantization with respect to the symbol alphabet $\mathcal{A}$. Inserting this bound into (20) yields

$$\begin{aligned}\Big\|\mathbf{q}_k^{(1)} - \mathbf{R}_k^{(11)}\mathbf{x}_k^{(1)} - \mathbf{R}_k^{(12)}\mathbf{x}_k^{(2)}\Big\|^2 &\geq \rho_k^2 \\ &\triangleq \sigma^2_{\min}\big(\mathbf{R}_k^{(11)}\big)\big\|\mathbf{b}_k - \mathcal{Q}_\mathcal{A}\{\mathbf{b}_k\}\big\|^2. \end{aligned}\tag{21}$$

Applying (21) to (17) finally leads to the necessary condition

$$\Big\|\mathbf{q}_k^{(2)} - \mathbf{R}_k^{(22)}\mathbf{x}_k^{(2)}\Big\|^2 \leq R^2 - \rho_k^2 \tag{22}$$

which is stronger than (18) and hence allows more aggressive tree pruning, thereby significantly reducing SD complexity. We note that $\sigma_{\min}\big(\mathbf{R}_k^{(11)}\big)$ and $\big(\mathbf{R}_k^{(11)}\big)^{-1}$, $k = 2, \ldots, M_\mathrm{T}$, can be precomputed prior to actually performing the tree search. The smallest singular value can be efficiently computed using the power method [21].

In order to illustrate the benefit of this particular SD modification, we consider the extreme case where $\alpha = 1$ (ZF). In this case $\mathbf{C}_\alpha = \mathbf{Q} = \mathbf{R} = \mathbf{I}$, $\sigma_{\min}\big(\mathbf{R}_k^{(11)}\big) = 1$, and $\mathbf{b}_k = \mathbf{q}_k^{(1)}$. Assuming that the initial sphere radius R is found via the ZF solution, i.e.,

$$\begin{aligned} R^2 &= \big\|\mathbf{q} - \mathcal{Q}_\mathcal{A}\{\mathbf{q}\}\big\|^2 \\ &= \Big\|\mathbf{q}_k^{(1)} - \mathcal{Q}_\mathcal{A}\{\mathbf{q}_k^{(1)}\}\Big\|^2 + \Big\|\mathbf{q}_k^{(2)} - \mathcal{Q}_\mathcal{A}\{\mathbf{q}_k^{(2)}\}\Big\|^2 \end{aligned}$$

the necessary condition (22) becomes

$$\begin{aligned}\Big\|\mathbf{q}_k^{(2)} - \mathbf{x}_k^{(2)}\Big\|^2 &\leq R^2 - \Big\|\mathbf{q}_k^{(1)} - \mathcal{Q}_\mathcal{A}\{\mathbf{q}_k^{(1)}\}\Big\|^2 \\ &\leq \Big\|\mathbf{q}_k^{(2)} - \mathcal{Q}_\mathcal{A}\{\mathbf{q}_k^{(2)}\}\Big\|^2. \end{aligned}\tag{23}$$

For any $\mathbf{x}_k^{(2)} \in \mathcal{A}^k$ different from the ZF solution, it holds with probability one that

$$\Big\|\mathbf{q}_k^{(2)} - \mathbf{x}_k^{(2)}\Big\| > \Big\|\mathbf{q}_k^{(2)} - \mathcal{Q}_\mathcal{A}\{\mathbf{q}_k^{(2)}\}\Big\| \tag{24}$$

which implies that (23) is violated with probability one whenever $\mathbf{x}$ differs from the ZF solution. Thus, the SD variant will visit only nodes corresponding to the ZF solution. The same can be shown to hold true for the Schnorr–Euchner strategy [2], [26], given that (22) is used for tree pruning. This implies that for $\alpha = 1$ the complexity of the SD variant is the same as that of ZF detection (neglecting the preprocessing), in spite of significant noise enhancement. This is in striking contrast to conventional SD whose complexity for $\alpha = 1$ can be even higher than that of ML decoding due to strong noise enhancement. In fact, our numerical simulations (see Section VI) confirmed that the above SD variant indeed has a complexity that decreases with increasing α.

D. Complexity of PSD Algorithm

We provide a short summary and assessment of the main computational steps required in the implementation of the PSD algorithm. We separately consider preprocessing tasks that are required once for each channel realization, and equalization and SD tasks that are required for each receive vector. The channel matrix $\mathbf{H}$ and the receive vector $\mathbf{r}$ constitute the detector input. For simplicity, we shall assume that $M_\mathrm{R} = M_\mathrm{T} = M$.

1) Preprocessing: In order to solve (15) using the above SD variant, we need to compute $\mathbf{W}_\alpha$ [appearing in (12)] and $\mathbf{C}_\alpha$. This can be accomplished via the SVD with $\mathcal{O}(M^3)$ operations. The computation of the QR decomposition of $\mathbf{C}_\alpha$, preferably implemented using Jacobi rotations [21], [28], requires $\mathcal{O}(M^3)$ operations as well. Finally, the minimum singular values $\sigma^2_{\min}\big(\mathbf{R}_k^{(11)}\big)$ and the inverses $\big(\mathbf{R}_k^{(11)}\big)^{-1}$, $k = 2, \ldots, M$, required for SD pruning can also be obtained

$$\begin{aligned}\Big\|\mathbf{q}_k^{(1)} - \mathbf{R}_k^{(11)}\mathbf{x}_k^{(1)} - \mathbf{R}_k^{(12)}\mathbf{x}_k^{(2)}\Big\|^2 &= \Big\|\mathbf{R}_k^{(11)}\Big[(\mathbf{R}_k^{(11)})^{-1}\mathbf{q}_k^{(1)} - \mathbf{x}_k^{(1)} - (\mathbf{R}_k^{(11)})^{-1}\mathbf{R}_k^{(12)}\mathbf{x}_k^{(2)}\Big]\Big\|^2 \\ &\geq \sigma^2_{\min}\big(\mathbf{R}_k^{(11)}\big)\big\|\mathbf{b}_k - \mathbf{x}_k^{(1)}\big\|^2 \end{aligned}\tag{20}$$

with complexity $\mathcal{O}(M^3)$ (assuming that the minimum singular values are obtained using the power method with a fixed number of iterations).

2) Equalization and Pruning: Each receive vector is first transformed according to $\mathbf{q} = \mathbf{Q}^H\mathbf{W}_\alpha^{-1}\mathbf{r}$ involving $\mathcal{O}(M^2)$ operations. In the SD tree search, the condition (22) needs to be checked for every visited node to see whether that node may be pruned; this can be done with $\mathcal{O}(M)$ operations using rank-one updates of certain intermediate quantities (see [15]). Unfortunately, the number of nodes visited by the SD variant is difficult to specify exactly. However, the arguments in Section IV-C and the numerical simulations in Section VI corroborate that the number of visited nodes is a decreasing function of α.

V. Diversity of PSD

In this section, we show that by varying the amount of preequalization via the parameter α, the diversity order of the proposed PSD scheme can be tuned to any value between $d_{\min} = M_{\mathrm{R}} - M_{\mathrm{T}} + 1$ (ZF detection) and $d_{\max} = M_{\mathrm{R}}$ (ML detection). This is accomplished by studying the average PEP. In our analysis, we assume an i.i.d. Rayleigh fading channel. However, [29] implies that the so-obtained diversity order applies as well to other fading distributions like spatially correlated Rayleigh and Ricean fading.

Assuming that $\mathbf{x}_1$ was transmitted (whence $\tilde{\mathbf{r}}_\alpha = \mathbf{C}_\alpha\mathbf{x}_1 + \tilde{\mathbf{n}}_\alpha$) and $\mathbf{x}_2 \neq \mathbf{x}_1$ is another candidate vector, the conditional PEP of PSD (cf. (15)) is given by

$$\begin{aligned} &P(\mathbf{x}_1 \rightarrow \mathbf{x}_2 \big| \mathbf{H}) \\ &\quad = \Pr\left\{||\check{\mathbf{r}}_\alpha - \mathbf{C}_\alpha\mathbf{x}_2||^2 \leq ||\check{\mathbf{r}}_\alpha - \mathbf{C}_\alpha\mathbf{x}_1||^2 \big| \mathbf{H}\right\} \\ &\quad = \Pr\left\{||\mathbf{C}_\alpha(\mathbf{x}_1 - \mathbf{x}_2) + \tilde{\mathbf{n}}_\alpha||^2 \leq ||\tilde{\mathbf{n}}_\alpha||^2 \big| \mathbf{H}\right\} \\ &\quad = \Pr\left\{||\mathbf{D}^{1-\alpha}\boldsymbol{\delta}||^2 \leq Z \big| \mathbf{H}\right\} \end{aligned} \tag{25}$$

where $\boldsymbol{\delta} = \mathbf{V}^H(\mathbf{x}_1 - \mathbf{x}_2)$, the random variable $Z = 2\mathrm{Re}\{(\mathbf{x}_1 - \mathbf{x}_2)^H\mathbf{C}_\alpha^H\mathbf{W}_\alpha^{-1}\mathbf{n}\} = 2\mathrm{Re}\{\boldsymbol{\delta}^H\mathbf{D}^{1-2\alpha}\mathbf{U}^H\mathbf{n}\}$ is distributed as $\mathcal{N}(0, 2\sigma_n^2||\mathbf{D}^{1-2\alpha}\boldsymbol{\delta}||^2)$, and we have used the factorizations of $\mathbf{C}_\alpha$ and $\mathbf{W}_\alpha^{-1}$ provided in Section III-B. We further develop (25) as

$$P(\mathbf{x}_1 \rightarrow \mathbf{x}_2 \big| \mathbf{H}) = \mathrm{Q}\left(\frac{\sqrt{\gamma_\alpha}}{\sigma_n}\right), \quad \text{with } \gamma_\alpha \triangleq \frac{1}{2}\frac{||\mathbf{D}^{1-\alpha}\boldsymbol{\delta}||^4}{||\mathbf{D}^{1-2\alpha}\boldsymbol{\delta}||^2}. \tag{26}$$

The average PEP is given by

$$\begin{aligned} P(\mathbf{x}_1 \rightarrow \mathbf{x}_2) &= \mathrm{E}_{\mathbf{H}}\left\{P(\mathbf{x}_1 \rightarrow \mathbf{x}_2 \big| \mathbf{H})\right\} \\ &= \mathrm{E}_{\gamma_\alpha}\left\{\mathrm{Q}\left(\frac{\sqrt{\gamma_\alpha}}{\sigma_n}\right)\right\}. \end{aligned} \tag{27}$$

It is difficult to obtain the statistics of γ_α in closed form. However, the diversity order is known to depend only on the behavior of γ_α in the vicinity of the origin. In particular, it can be shown (cf. [30] and [31, Ch. 3]) that

$$d_\alpha = \lim_{\epsilon \rightarrow 0} \frac{\log \Pr\{\gamma_\alpha \leq \epsilon\}}{\log \epsilon}. \tag{28}$$

Following [31], we refer to channel realizations for which γ_α is on the order of ϵ (or σ_n^2) as *deep fades*. Since $\boldsymbol{\Lambda} = \mathbf{D}^2$, the factor γ_α may be expressed explicitly in terms of the eigenvalues and eigenvectors[1] of the Gram matrix $\mathbf{G}$, i.e.,

$$\gamma_\alpha = \frac{1}{\nu}\frac{\left(\mathbf{u}^H\boldsymbol{\Lambda}^{1-\alpha}\mathbf{u}\right)^2}{\mathbf{u}^H\boldsymbol{\Lambda}^{1-2\alpha}\mathbf{u}} \tag{29}$$

where $\nu = 2||\boldsymbol{\delta}||$ and $\mathbf{u} = (u_1 \ldots u_{M_{\mathrm{T}}})^T \triangleq \boldsymbol{\delta}/||\boldsymbol{\delta}||$. Note that $||\mathbf{u}|| = 1$ and $\mathbf{u}$ is uniformly distributed over the unit sphere. The events that dominate the probability that $\gamma_\alpha \leq \epsilon$ will be termed *typical errors* (cf. [32]). Note, however, that different from [32] the typical errors in our case will depend both on $\boldsymbol{\Lambda}$ *and* $\mathbf{u}$.

A rigorous evaluation of (28) is provided in Appendix B. Below, we provide a heuristic discussion of the relevant events that induce deeps fades. To this end, we use $\gamma_\alpha = \Theta(\epsilon^\delta)$ to denote that γ_α is "on the order of ϵ^δ" when $\epsilon > 0$ is small[2]. Thus, a deep fade occurs for $\gamma_\alpha = \Theta(\epsilon)$. Consider first the event that

$$\lambda_1 = \Theta(\epsilon), \quad \lambda_2, \ldots, \lambda_{M_{\mathrm{T}}} = \Theta(1) \tag{30a}$$

$$|u_1|^2 = \Theta(1), \quad |u_2|^2, \ldots, |u_{M_{\mathrm{T}}}|^2 = \Theta(\epsilon^{1-\alpha}). \tag{30b}$$

It follows that

$$\mathbf{u}^H\boldsymbol{\Lambda}^{1-\alpha}\mathbf{u} = \sum_{i=1}^{M_{\mathrm{T}}} \underbrace{|u_i|^2\lambda_i^{1-\alpha}}_{\Theta(\epsilon^{1-\alpha})} = \Theta(\epsilon^{1-\alpha})$$

and

$$\left(\mathbf{u}^H\boldsymbol{\Lambda}^{1-\alpha}\mathbf{u}\right)^2 = \Theta(\epsilon^{2-2\alpha}). \tag{31}$$

At the same time

$$\begin{aligned} \mathbf{u}^H\boldsymbol{\Lambda}^{1-2\alpha}\mathbf{u} &= \underbrace{|u_1|^2\lambda_1^{1-2\alpha}}_{\Theta(\epsilon^{1-2\alpha})} + \sum_{i=2}^{M_{\mathrm{T}}} \underbrace{|u_i|^2\lambda_i^{1-2\alpha}}_{\Theta(\epsilon^{1-\alpha})} \\ &= \Theta(\epsilon^{1-2\alpha}) \end{aligned} \tag{32}$$

where the last equality follows since for small ϵ there is $\epsilon^{1-2\alpha} \geq \epsilon^{1-\alpha}$. In view of (29), (31) and(32) imply that

$$\gamma_\alpha = \Theta(\epsilon).$$

We conclude that the events in (30) are sufficient for the occurrence of a deep fade. Since $\mathbf{u}$ and $\boldsymbol{\Lambda}$ are independent due to the i.i.d. assumption on $\mathbf{H}$ [33], it follows that the probability that (30a) and (30b) hold simultaneously is given by the product of the individual probabilities.

The probability of (30a) is $\Theta(\epsilon^{d_{\min}})$ (cf. [32, Eq. (15)]). Furthermore, it can be shown that the probability of (30b) is $\Theta(\epsilon^{(1-\alpha)(M_{\mathrm{T}}-1)})$. As a support of this statement, note that $S \triangleq \sum_{i=2}^{M_{\mathrm{T}}}|u_i|^2$ is beta distributed with probability density function $f_S(s) = (M_{\mathrm{T}} - 1)s^{M_{\mathrm{T}}-2}$ for $s \in [0, 1]$ [34]. Thus,

$$\begin{aligned} &\Pr\left\{S \leq \epsilon^{1-\alpha}\right\} \\ &\qquad = (M_{\mathrm{T}} - 1)\int_0^{\epsilon^{1-\alpha}} x^{M_{\mathrm{T}}-2}dx = \Theta(\epsilon^{(1-\alpha)(M_{\mathrm{T}}-1)}). \end{aligned}$$

[1]From now on, we assume that the eigenvalues of the Gram matrix are sorted in ascending order.

[2]Formally, $X = \Theta(\epsilon^\delta)$ means that there exist constants $C > c > 0$ and $\epsilon_0 > 0$ independent of ϵ such that $c\epsilon^\delta \leq X \leq C\epsilon^\delta$ for $0 < \epsilon < \epsilon_0$. Similarly, $X = O(\epsilon^\delta)$ is used to denote the one sided inequality $X \leq C\epsilon^\delta$.

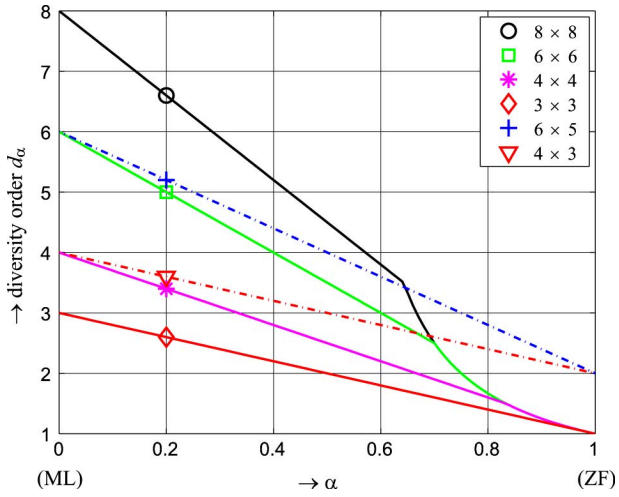

Fig. 2. Diversity order of PSD versus α for various antenna configurations $M_{\mathrm{R}} \times M_{\mathrm{T}}$. ML and ZF detection correspond to $\alpha = 0$ and $\alpha = 1$, respectively.

As $S \leq \epsilon^{1-\alpha}$ implies that $|u_i|^2 \leq \epsilon^{1-\alpha}$ for $i = 2, \ldots, M_{\mathrm{T}}$, and $|u_1|^2 \geq 1 - \epsilon^{1-\alpha} = \Theta(1)$ since $\|\mathbf{u}\|^2 = 1$, it follows that the probability of (30b) is $O(\epsilon^{(1-\alpha)(M_{\mathrm{T}}-1)})$. Establishing that this bound is tight proves that (30b) occurs with probability $\Theta(\epsilon^{(1-\alpha)(M_{\mathrm{T}}-1)})$. The probability that (30a) and (30b) are simultaneously satisfied is thus $\Theta(\epsilon^{d_\alpha^{(1)}})$ where

$$\begin{aligned} d_\alpha^{(1)} \triangleq & (M_{\mathrm{R}} - M_{\mathrm{T}} + 1) + (1-\alpha)(M_{\mathrm{T}} - 1) \\ = & \alpha d_{\min} + (1-\alpha)\, d_{\max}. \end{aligned} \tag{33}$$

The diversity order d_α is thus upper bounded according to

$$d \leq d_\alpha^{(1)}. \tag{34}$$

Note however that the inequality is not necessarily tight as (30) are only sufficient, not necessary, conditions for a deep fade. Nevertheless, it is interesting to note that (33) represents a convex combination of ML and ZF diversity. Therefore, (34) is known to be tight at least for $\alpha = 0$ and $\alpha = 1$. We will show later that for certain M_{R} and M_{T}, (34) is tight over the entire range $\alpha \in [0, 1]$.

However, for some M_{R}, M_{T}, and $\alpha > 1/2$, another possible cause of deep fades can become typical and dominate the error probability. The corresponding joint event is given by

$$\lambda_1 = \Theta\big(\epsilon^{1/2\alpha - 1}\big), \quad \lambda_2, \ldots, \lambda_{M_{\mathrm{T}}} = \Theta(1) \tag{35a}$$

$$|u_1|^2, |u_2|^2, \ldots, |u_{M_{\mathrm{T}}}|^2 = \Theta(1). \tag{35b}$$

It is straightforward to ascertain that the conditions in (35) are sufficient for a deep fade by verifying that

$$\big(\mathbf{u}^H \mathbf{\Lambda}^{1-\alpha} \mathbf{u}\big)^2 = \Theta(1), \quad \big(\mathbf{u}^H \mathbf{\Lambda}^{1-2\alpha} \mathbf{u}\big)^{-1} = \Theta(\epsilon).$$

The probability of (35a) is $\Theta\big(\epsilon^{(M_{\mathrm{R}} - M_{\mathrm{T}} + 1)/(2\alpha - 1)}\big)$, and the probability of (35b) is $\Theta(1)$, yielding a joint probability of $\Theta\big(\epsilon^{d_\alpha^{(2)}}\big)$ where

$$d_\alpha^{(2)} \triangleq \frac{d_{\min}}{2\alpha - 1}. \tag{36}$$

It follows that $d_\alpha \leq \min(d_\alpha^{(1)}, d_\alpha^{(2)})$ for $\alpha > 1/2$. As it turns out, the two types of error events discussed above are the only ones that can become typical (in the sense that they dominate the overall probability of error) and hence completely determine PSD diversity. This is formally stated by the following theorem.

Theorem 1: The diversity of PSD is given by

$$d_\alpha = \begin{cases} \alpha d_{\min} + (1-\alpha) d_{\max}, & \text{for } 0 \leq \alpha \leq \alpha_0 \\ \dfrac{d_{\min}}{2\alpha - 1}, & \text{for } \alpha_0 \leq \alpha \leq 1 \end{cases}$$

where $\alpha_0 \triangleq \min\big(1, M_{\mathrm{R}}/(M_{\mathrm{T}} - 1) - 1/2\big) > 1/2$.

Proof: See Appendix B.

According to Theorem 1, the design parameter α allows us to scale the diversity order of PSD continuously between the diversity order $d_{\max}$ of the ML detector and the diversity order $d_{\min}$ of the ZF detector. In fact, any target diversity d order between $d_{\min}$ and $d_{\max}$ can be achieved by choosing the pre-equalization parameter as

$$\alpha = \min\left(\frac{d_{\max} - d}{M_{\mathrm{T}} - 1}, \frac{d + d_{\min}}{2d}\right).$$

While [35] conjectured that the diversity order of the proposed PSD detector is linear in α within the whole interval $[0, 1]$, this is actually true only for antenna configurations satisfying

$$M_{\mathrm{R}} \geq \frac{3}{2}(M_{\mathrm{T}} - 1). \tag{37}$$

If (37) is not satisfied, there is a threshold $\alpha_0 < 1$ above which the diversity order decays nonlinearly. Examples for the diversity order of PSD for various antenna configurations are shown in Fig. 2. We emphasize that Theorem 1 applies to uncoded systems. Taking into account an outer error-correcting code may change the overall system diversity.

VI. Simulation Results

In this section, we provide numerical results illustrating the performance and complexity of the proposed PSD receiver. We simulated an uncoded 6×6 MIMO spatial multiplexing system with a 16-QAM symbol alphabet. The SD variant is implemented in the complex domain using the Schnorr–Euchner strategy as described in Section IV-C. All results were obtained by averaging with respect to channel, noise, and data.

Fig. 3(a) shows symbol error rate (SER) versus SNR for $\alpha \in \{0, 1/4, 1/2, 3/4, 1\}$. Recall that $\alpha = 0$ and $\alpha = 1$ correspond to ML and ZF, respectively. It is seen that the diversity of PSD indeed scales with α according to Theorem 1. Note that in this case $\alpha_0 = 0.7$, i.e., the point $\alpha = 0.75$ is in the regime where diversity decays nonlinearly (see Fig. 2).

Fig. 3(b) depicts the average and the 90% percentile of the number of nodes visited by the SD variant versus the pre-equalization parameter α for an SNR of 18 dB. Here, the SD variant examines the nodes in the order of increasing $\big\|\mathbf{q}_k^{(2)} - \mathbf{R}_k^{(22)} \mathbf{x}_k^{(2)}\big\|^2$. The average number of nodes visited by the standard SD, shown for sake of comparison, increases dramatically for $\alpha > 1/2$. This undesired behavior is the reason why we propose to use the SD variant. It is seen that in this case

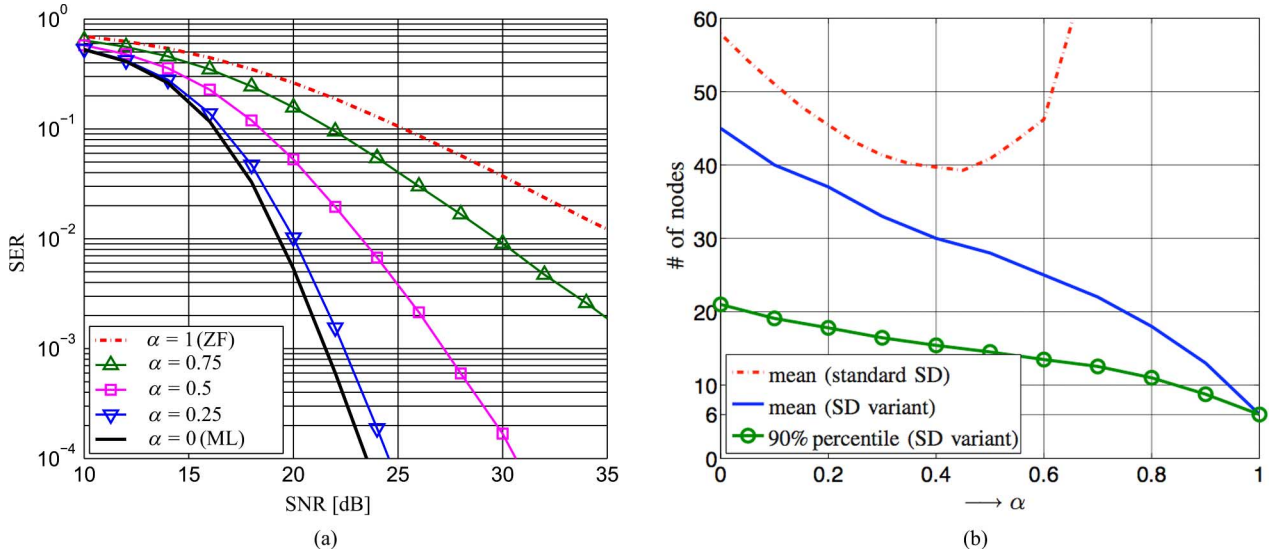

Fig. 3. (a) SER versus SNR of PSD with various α and (b) complexity (average and percentile of visited nodes) versus α for $M_{\mathrm{T}} = M_{\mathrm{R}} = 6$ and 16-QAM symbol alphabet.

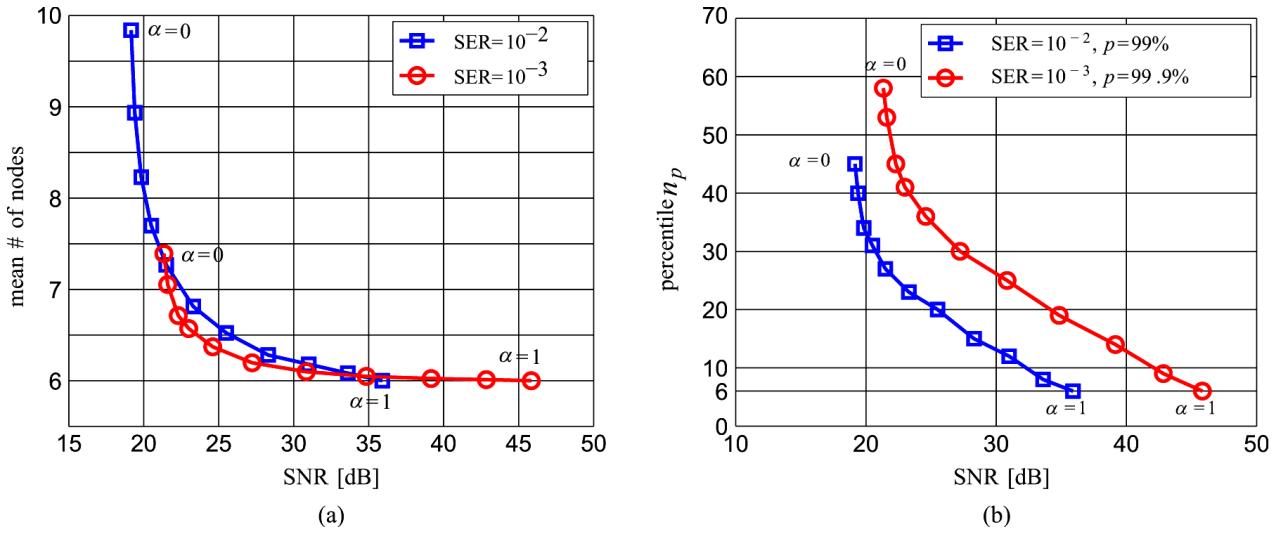

Fig. 4. (a) Mean and (b) percentile of the number of visited nodes versus the SNR required to achieve a certain target SER with different α for $M_{\mathrm{T}} = M_{\mathrm{R}} = 6$ and 16-QAM symbol alphabet.

the number of nodes visited indeed decreases with increasing pre-equalization parameter α. We note that in this example the SD tree has six layers and hence the minimum number of visited nodes equals 6. This complexity is indeed obtained with $\alpha = 1$ (ZF detection). Fig. 3(a) and (b) illustrate that the PSD scheme indeed provides a continuous tradeoff between diversity and complexity.

A different perspective of the diversity-complexity tradeoff is provided by Fig. 4, which shows the number of nodes visited by the SD variant versus the SNR required to achieve target SERs of 10^{-2} and 10^{-3} with various degrees of pre-equalization α (α is increased from 0 to 1 in steps of $1/10$, each value corresponding to a marker). Fig. 4(a) shows the average number of visited nodes versus required SNR. For α up to about $1/2$, complexity is seen to decrease substantially without dramatic increase in the required SNR, whereas for larger α further complexity savings are only possible with larger SNR penalty. Here, curves for different target SERs should only be compared for a fixed α since each α refers to a different receiver. We note that other detectors (e.g., [36]) may be able to better exploit the improved channel condition number for large α, resulting in a more favorable performance-complexity tradeoff in that regime. Fig. 4(b) shows the percentiles n_p of the number of nodes visited versus the required SNR. Here, the SD examines the nodes in the order of increasing $\left\|\mathbf{q}_k^{(2)} - \mathbf{R}_k^{(22)}\mathbf{x}_k^{(2)}\right\|^2 + \rho_k^2$ [cf. (22)], which allows to reduce complexity even more. The percentiles are chosen according to $p = 1 - \mathrm{SER}$. With this choice, *decoding outages* that would result when the SD variant is terminated early at the specified percentile level occur with a probability equal to SER and hence will not significantly affect overall system performance. These results show that n_p, too, decays with increasing α with small initial SNR loss and somewhat larger SNR loss for larger α.

As seen in Fig. 4(b) for $\mathrm{SER} = 10^{-3}$, the complexity can be reduced approximately by 30% ($\alpha = 0.25$) without much loss in diversity order ($d = 4.75$ with a loss of 1.25) and the SNR gap to ML detection is approximately 1 dB (see Fig. 3). Both parts of Fig. 4 clearly illustrate that the pre-equalization parameter α al-

lows to scale complexity at a certain SNR expense (determined by the diversity loss quantified in Theorem 1). This corroborates that the proposed PSD scheme indeed allows a tradeoff between diversity order and complexity savings.

VII. Conclusion

Motivated by a unified formulation of ML and ZF detection, we proposed a novel hard-output MIMO detector which consists of a linear equalizer that partially eliminates MIMO interference and improves the channel condition number, followed by a mismatched ML detector, which ignores the noise correlation resulting from the first stage. The second stage is implemented using a variant of the SD suited for low SNR. The overall scheme is referred to as PSD and allows for significant complexity savings at the expense of a certain diversity loss. Appropriate tuning of the amount of equalization in the first stage results in a continuous tradeoff between complexity reduction and diversity order. Hence, our PSD scheme can be adjusted to any desired level of performance or complexity. Since practical MIMO systems employ channel coding, a soft-input soft-output extension of PSD for iterative detection and decoding is an interesting research topic. Among the main competitors in such a setup are iterative receivers based on interference cancellation.

Appendix A
Impact of α on the SNR

We prove that the instantaneous SNR is a strictly decreasing function in α (unless $\kappa(\mathbf{H})=1$ in which case it is constant). To this end, note that the instantaneous SNR in (19) can we written as

$$\mathrm{snr}_\alpha = \frac{c}{\sigma_n^2}\frac{\sum_{i=1}^{M_\mathrm{T}} \lambda_i^{1-\alpha}}{\sum_{i=1}^{M_\mathrm{T}} \lambda_i^{-\alpha}}$$

where c is a positive constant. We proceed to show that the first derivative of $\ln(\mathrm{snr}_\alpha)$ is strictly less than zero (or equal to zero when $\lambda_i=\lambda_j$ for all i and j). This implies that snr_α is strictly decreasing since the logarithm is a strictly increasing function. We have

$$\begin{aligned}\frac{d\ln \mathrm{snr}_\alpha}{d\alpha} &= -\frac{\sum_{i=1}^{M_\mathrm{T}} \lambda_i^{(1-\alpha)}\ln\lambda_i}{\sum_{i=1}^{M_\mathrm{T}} \lambda_i^{(1-\alpha)}} + \frac{\sum_{i=1}^{M_\mathrm{T}} \lambda_i^{-\alpha}\ln\lambda_i}{\sum_{i=1}^{M_\mathrm{T}} \lambda_i^{-\alpha}} \\ &= \frac{\sum_{i=1}^{M_\mathrm{T}}\sum_{j=1}^{M_\mathrm{T}} \lambda_j^{-\alpha}\lambda_i^{1-\alpha}\ln\left(\frac{\lambda_j}{\lambda_i}\right)}{\left(\sum_{i=1}^{M_\mathrm{T}} \lambda_i^{(1-\alpha)}\right)\left(\sum_{i=1}^{M_\mathrm{T}} \lambda_i^{-\alpha}\right)}. \end{aligned} \tag{38}$$

Using the inequality $\ln x \le x-1$ (with equality if and only if $x=1$), the numerator in (38) can be upper bounded as

$$\begin{aligned}\sum_{i=1}^{M_\mathrm{T}}\sum_{j=1}^{M_\mathrm{T}} \lambda_j^{-\alpha}\lambda_i^{1-\alpha}\ln\left(\frac{\lambda_j}{\lambda_i}\right) &\le \sum_{i=1}^{M_\mathrm{T}}\sum_{j=1}^{M_\mathrm{T}} \lambda_j^{-\alpha}\lambda_i^{1-\alpha}\left(\frac{\lambda_j}{\lambda_i}-1\right) \\ &= \sum_{i=1}^{M_\mathrm{T}}\sum_{j=1}^{M_\mathrm{T}} \lambda_j^{1-\alpha}\lambda_i^{-\alpha} - \lambda_j^{-\alpha}\lambda_i^{1-\alpha} = 0.\end{aligned}$$

Since the denominator of (38) is positive, this proves that the instantaneous SNR is a strictly monotonically decreasing function of α, unless $\lambda_i=\lambda_j$ for all i,j in which case snr_α is constant.

Appendix B
Proof of Theorem 1

Based on (28), it follows that in order to compute the diversity order of PSD it is sufficient to compute the probability that $\gamma_\alpha \le \epsilon$ as ϵ tends to zero. The condition that $\gamma_\alpha \le \epsilon$ may equivalently be written as

$$\left(\mathbf{u}^H\mathbf{\Lambda}^{1-\alpha}\mathbf{u}\right)^2 \le \epsilon\nu\,\mathbf{u}^H\mathbf{\Lambda}^{1-2\alpha}\mathbf{u}$$

or

$$\left(\sum_{i=1}^{M_T}\mu_i\lambda_i^{1-\alpha}\right)^2 \le \epsilon\nu\sum_{i=1}^{M_T}\mu_i\lambda_i^{1-2\alpha} \tag{39}$$

where $\mu_i=|u_i|^2$ and u_i is the ith entry of $\mathbf{u}$. To simplify (39), note that

$$\begin{aligned}\max_i \mu_i^2\lambda_i^{2(1-\alpha)} &\le \left(\sum_{i=1}^{M_T}\mu_i\lambda_i^{1-\alpha}\right)^2 \\ &\le M_T^2\max_i \mu_i^2\lambda_i^{2(1-\alpha)}\end{aligned}$$

and

$$\max_i \mu_i\lambda_i^{1-2\alpha} \le \sum_{i=1}^{M_T}\mu_i\lambda_i^{1-2\alpha} \le M_T\max_i \mu_i\lambda_i^{1-2\alpha}.$$

Thus, the bound given by

$$\max_i \mu_i^2\lambda_i^{2(1-\alpha)} \le \epsilon\nu M_T\max_i \mu_i\lambda_i^{1-2\alpha} \tag{40}$$

is looser than (39) and

$$M_T^2\max_i \mu_i^2\lambda_i^{2(1-\alpha)} \le \epsilon\nu\max_i \mu_i\lambda_i^{1-2\alpha} \tag{41}$$

is tighter than (39). Proceed by introducing the variable transformations given by [32]

$$\xi_i \triangleq \frac{\ln\lambda_i}{\ln\epsilon} \Leftrightarrow \lambda_i = \epsilon^{\xi_i} \tag{42}$$

and

$$\zeta_i \triangleq \frac{\ln\mu_i}{\ln\epsilon} \Leftrightarrow \mu_i = \epsilon^{\zeta_i} \tag{43}$$

for $i = 1, \ldots, M_T$. In the transformed coordinates, (40) becomes

$$2 \min_i \left[\zeta_i + (1-\alpha)\xi_i\right] \geq 1 + \min_i \left[\zeta_i + (1-2\alpha)\xi_i\right] + \frac{\ln \nu M_T}{\ln \epsilon}$$

and (41) becomes

$$2 \min_i \left[\zeta_i + (1-\alpha)\xi_i\right] \geq 1 + \min_i \left[\zeta_i + (1-2\alpha)\xi_i\right] + \frac{\ln \nu M_T^{-2}}{\ln \epsilon}.$$

Note also that since

$$\lim_{\epsilon \longrightarrow 0} \frac{\ln \nu M_T}{\ln \epsilon} = \lim_{\epsilon \longrightarrow 0} \frac{\ln \nu M_T^{-2}}{\ln \epsilon} = 0$$

it follows that these bounds become tighter as ϵ tends to zero. Let

$$\mathcal{O}_\delta \triangleq \Big\{(\boldsymbol{\xi}, \boldsymbol{\zeta}) \mid 2 \min_i \left[\zeta_i + (1-\alpha)\xi_i\right] \geq 1 + \min_i \left[\zeta_i + (1-2\alpha)\xi_i\right] - \delta\Big\}$$

where $\boldsymbol{\xi} = (\xi_1, \ldots, \xi_{M_T})$ and $\boldsymbol{\zeta} = (\zeta_1, \ldots, \zeta_{M_T})$. Then, for sufficiently small $\epsilon > 0$, it follows that

$$\Pr\{\gamma_\alpha \leq \epsilon\} \leq \Pr\{(\boldsymbol{\xi}, \boldsymbol{\zeta}) \in \mathcal{O}_\delta\} \tag{44}$$

for any $\delta > 0$. Similarly, for sufficiently small $\epsilon > 0$, it also follows that

$$\Pr\{\gamma_\alpha \leq \epsilon\} \geq \Pr\{(\boldsymbol{\xi}, \boldsymbol{\zeta}) \in \mathcal{O}_\delta\} \tag{45}$$

for any $\delta < 0$. In the following, it will be shown how to compute these probabilities using large deviations techniques [16].

A. Large Deviations

By the term *rate function* we refer to a lower semicontinuous mapping $I : \mathbb{R}^n \mapsto [0, \infty]$. For a given set $\mathcal{A}$, let $\mathcal{A}^o$ denote the interior of $\mathcal{A}$ and let $\bar{\mathcal{A}}$ denote the closure of $\mathcal{A}$. A family of random variables (or vectors), $\boldsymbol{\nu}_\epsilon \in \mathbb{R}^n$, parameterized by $\epsilon > 0$ are said to satisfy the *large deviation principle* (LDP) with rate function $I(\boldsymbol{\nu})$ if

$$\inf_{\boldsymbol{\nu} \in \mathcal{A}^o} I(\boldsymbol{\nu}) \geq \limsup_{\epsilon \longrightarrow 0} \frac{\ln \Pr\{\boldsymbol{\nu}_\epsilon \in \mathcal{A}\}}{\ln \epsilon} \geq \liminf_{\epsilon \longrightarrow 0} \frac{\ln \Pr\{\boldsymbol{\nu}_\epsilon \in \mathcal{A}\}}{\ln \epsilon} \geq \inf_{\boldsymbol{\nu} \in \bar{\mathcal{A}}} I(\boldsymbol{\nu}) \tag{46}$$

for any measurable set $\mathcal{A} \subset \mathbb{R}^n$ [16]. In particular, whenever

$$\inf_{\boldsymbol{\nu} \in \mathcal{A}^o} I(\boldsymbol{\nu}) = \inf_{\boldsymbol{\nu} \in \bar{\mathcal{A}}} I(\boldsymbol{\nu}) = I_{\mathcal{A}} \tag{47}$$

it follows that

$$\lim_{\epsilon \longrightarrow 0} \frac{\ln \Pr\{\boldsymbol{\nu}_\epsilon \in \mathcal{A}\}}{\ln \epsilon} = I_{\mathcal{A}}.$$

A set $\mathcal{A}$ satisfying (47) is referred to as an *I-continuity* set [16].

Consider $\boldsymbol{\xi} = (\xi_1, \ldots, \xi_{M_T})$ and $\boldsymbol{\zeta} = (\zeta_1, \ldots, \zeta_{M_T})$ where ξ_i and ζ_i is defined according to (42) and (43) respectively. Note also that $\boldsymbol{\xi} = \boldsymbol{\xi}_\epsilon$ and $\boldsymbol{\zeta} = \boldsymbol{\zeta}_\epsilon$ represent a family of random variables parameterized by $\epsilon \in (0, 1)$. In [32] it was shown that $\boldsymbol{\xi}$ satisfies the LDP with rate function

$$I_\xi(\boldsymbol{\xi}) \triangleq \begin{cases} \sum_{i=1}^{M_T} (M_R - M_T + 2i - 1)\xi_i, & \text{if } \xi_1 \geq \xi_2 \geq \cdots \geq \xi_{M_T} \geq 0 \\ \infty, & \text{otherwise.} \end{cases} \tag{48}$$

This rate function was used in [32] to compute the outage probability for the MIMO channel considered, see in particular [32, Theorem 4].

In Appendix B-C it is shown that $\boldsymbol{\zeta}$ satisfies the LDP with rate function

$$I_\zeta(\boldsymbol{\zeta}) \triangleq \begin{cases} \sum_{i=1}^{M_T} \zeta_i, & \text{if } \zeta_i \geq 0 \text{ for all } i \text{ and } \zeta_i = 0 \text{ for some } i, \\ \infty, & \text{otherwise.} \end{cases} \tag{49}$$

Further, since $\boldsymbol{\xi}$ and $\boldsymbol{\zeta}$ are independent (and satisfy some technical conditions), it follows that the pair $(\boldsymbol{\xi}, \boldsymbol{\zeta})$ satisfy the LDP with rate function

$$I(\boldsymbol{\xi}, \boldsymbol{\zeta}) \triangleq I_\xi(\boldsymbol{\xi}) + I_\zeta(\boldsymbol{\zeta}) \tag{50}$$

see [16, Exercise 4.2.7]. By the LDP of $I(\boldsymbol{\xi}, \boldsymbol{\zeta})$, combined with (44) and (45), it follows that

$$\liminf_{\epsilon \longrightarrow 0} \frac{\ln \Pr\{\gamma_\alpha \leq \epsilon\}}{\ln \epsilon} \geq \inf_{(\boldsymbol{\xi}, \boldsymbol{\zeta}) \in \bar{\mathcal{O}}_\delta} I(\boldsymbol{\xi}, \boldsymbol{\zeta}) \tag{51}$$

for any $\delta > 0$ and that

$$\limsup_{\epsilon \longrightarrow 0} \frac{\ln \Pr\{\gamma_\alpha \leq \epsilon\}}{\ln \epsilon} \leq \inf_{(\boldsymbol{\xi}, \boldsymbol{\zeta}) \in \mathcal{O}_\delta^o} I(\boldsymbol{\xi}, \boldsymbol{\zeta}). \tag{52}$$

for any $\delta < 0$. However, it is fairly straightforward to see that $\mathcal{O}_\delta$ is an I-continuity set and that the right-hand sides of (51) and (52) are continuous in δ. Therefore,

$$\lim_{\epsilon \longrightarrow 0} \frac{\ln \Pr\{\gamma_\alpha \leq \epsilon\}}{\ln \epsilon} = \inf_{(\boldsymbol{\xi}, \boldsymbol{\zeta}) \in \mathcal{O}} I(\boldsymbol{\xi}, \boldsymbol{\zeta}) \tag{53}$$

where $\mathcal{O} \triangleq \mathcal{O}_0$ or equivalently

$$\mathcal{O} = \{(\boldsymbol{\xi}, \boldsymbol{\zeta}) \mid 2 \min_i \left[\zeta_i + (1-\alpha)\xi_i\right] \geq 1 + \min_i \left[\zeta_i + (1-2\alpha)\xi_i\right]\}. \tag{54}$$

In short, the PSD diversity is given by the minimum appearing on the right-hand side of (53). All that remains to be proven is that the minimum of (53) coincides with what is given in Theorem 1.

B. Finding the Minimum

The objective of this section is to compute

$$d = \inf_{(\boldsymbol{\xi}, \boldsymbol{\zeta}) \in \mathcal{O}} I(\boldsymbol{\xi}, \boldsymbol{\zeta}). \tag{55}$$

Since $\mathcal{O}$ is closed it follows that the minimum is attained for some pair $(\boldsymbol{\xi}^\star, \boldsymbol{\zeta}^\star) \in \mathcal{O}$. It is straightforward to see that $d < \infty$ which implies that $\boldsymbol{\xi}^\star$ and $\boldsymbol{\zeta}^\star$ must satisfy $I_\xi(\boldsymbol{\xi}^\star) < \infty$ and $I_\zeta(\boldsymbol{\zeta}^\star) < \infty$. Specifically, we have

$$\xi_1^\star \geq \xi_2^\star \geq \cdots \geq \xi_{M_T}^\star \geq 0 \tag{56}$$

and

$$\zeta_1^\star, \zeta_2^\star, \ldots, \zeta_{M_T}^\star \geq 0 \tag{57}$$

with $\zeta_k^\star = 0$ for some k [cf. (49)]. Now, consider the constraint imposed by $\mathcal{O}$ (54), namely

$$2 \min_i \left[\zeta_i^\star + (1-\alpha)\xi_i^\star\right] \geq 1 + \min_i \left[\zeta_i^\star + (1-2\alpha)\xi_i^\star\right] \tag{58}$$

or equivalently

$$2\zeta_k^\star + 2(1-\alpha)\xi_k^\star \geq 1 + \min_i \left[\zeta_i^\star + (1-2\alpha)\xi_i^\star\right] \tag{59}$$

for $k = 1, \ldots, M_T$. Since $\xi_1^\star \geq \xi_i^\star$ (cf. (49)) for all i it follows that

$$\min_i \left[\zeta_i^\star + (1-2\alpha)\xi_i^\star\right] \geq \min_i \left[\zeta_i^\star + (1-\alpha)\xi_i^\star\right] - \alpha\xi_1^\star.$$

Substituting this back into (58) yields

$$\min_i \left[\zeta_i^\star + (1-\alpha)\xi_i^\star\right] \geq 1 - \alpha\xi_1^\star.$$

In particular, for $i = 1$, it follows that

$$\zeta_1^\star + (1-\alpha)\xi_1^\star \geq 1 - \alpha\xi_1^\star \tag{60}$$

which implies $\zeta_1^\star + \xi_1^\star \geq 1$.

We proceed by proving that $\zeta_1^\star = 0$. To this end, we will assume that $\zeta_1^\star > 0$ and show that this leads to a contradiction. The assumption that $\zeta_1^\star > 0$ implies that there is a $k > 1$ for which $\zeta_k^\star = 0$ holds [cf. (49) and (57)]. Starting from (60), and letting k be such that $\zeta_k^\star = 0$, we write

$$\begin{aligned} 2(\zeta_1^\star + (1-\alpha)\xi_1^\star) &> 2(\zeta_k^\star + (1-\alpha)\xi_k^\star) \\ &\geq 1 + \min_i[\zeta_i^\star + (1-2\alpha)\xi_i^\star] \end{aligned}$$

where we used (59) and the assumption that $\zeta_1^\star > \zeta_k^\star = 0$ and that $\xi_1^\star \geq \xi_k^\star$ [cf. (56)]. This however implies that $\zeta_1^\star$ could be reduced without violating the constraint in (57) and (58) and since this would reduce $I_\zeta(\boldsymbol{\zeta}^\star)$ it contradicts the optimality of $(\boldsymbol{\xi}^\star,\ \boldsymbol{\zeta}^\star)$. Therefore, the assumption that $\zeta_1^\star > 0$ is false and we can state $\zeta_1^\star = 0$. Further, it also follows that $\xi_1^\star \geq 1$ since $\zeta_1^\star + \xi_1^\star \geq 1$ and from (59) we can state

$$2(1-\alpha)\xi_1^\star \geq 1 + \min_i \left[\zeta_i^\star + (1-2\alpha)\xi_i^\star\right]. \tag{61}$$

We proceed by proving

$$(1-2\alpha)\xi_1^\star = \min_i \left[\zeta_i^\star + (1-2\alpha)\xi_i^\star\right]. \tag{62}$$

When $1 - 2\alpha \leq 0$ this follows directly since

$$\zeta_i^\star + (1-2\alpha)\xi_i^\star \geq (1-2\alpha)\xi_1^\star$$

for all i due to $\zeta_i^\star \geq 0$, $\xi_1^\star \geq \xi_i^\star$ and $\zeta_1 = 0$. Equality is obtained for $i = 1$ which proves (62) in the case where $1 - 2\alpha \leq 0$. For the opposite case, i.e., $1 - 2\alpha > 0$, we assume a strict inequality in (61) i.e.,

$$2(1-\alpha)\xi_1^\star > 1 + \min_i \left[\zeta_i^\star + (1-2\alpha)\xi_i^\star\right] \tag{63}$$

and argue that this leads to a contradiction. To this end let k be and integer such that $\xi_1^\star = \xi_2^\star = \cdots = \xi_k^\star > \xi_{k+1}^\star \geq 0$. If no such k exists, i.e., if $\xi_1^\star = \cdots = \xi_{M_T}^\star$, we let $k = M_T$ and note that $\xi_1^\star = \xi_{M_T}^\star > 0$ is implied by (59). In either case, it follows that $\xi_k^\star$ may be reduced without violating (56). Further, as $\xi_1^\star = \xi_k^\star$ it follows by the assumption in (63) that

$$2(1-\alpha)\xi_k^\star > 1 + \min_i \left[\zeta_i^\star + (1-2\alpha)\xi_i^\star\right].$$

This however implies that also (59) [or equivalently (58)] is satisfied with strict inequality. Thus, $\xi_k^\star$ may be reduced, violating the optimality of $(\boldsymbol{\xi}^\star, \boldsymbol{\zeta}^\star)$. We conclude that the assumed strict inequality in (63) is false, hence (62) holds true.

Inserting (62) into (59) yields

$$\zeta_i^\star + (1-\alpha)\xi_i^\star \geq \frac{1}{2}(1 + (1-2\alpha)\xi_1^\star)$$

for $i = 1, \ldots, M_T$. Combining this with the trivial bound $\zeta_i^\star + (1-\alpha)\xi_i^\star \geq 0$ which follows from $\zeta_i^\star, \xi_i^\star \geq 0$ and $(1-\alpha) \geq 0$ yields

$$\zeta_i^\star + (1-\alpha)\xi_i^\star \geq \frac{1}{2}(1 + (1-2\alpha)\xi_1^\star)^+ \tag{64}$$

where $(a)^+ = \max(a, 0)$.

Now, using (64) it follows that

$$\begin{aligned} d &= \sum_{i=1}^{M_T}(M_R - M_T + 2i - 1)\xi_i^\star + \sum_{i=2}^{M_T}\zeta_i^\star \\ &= (M_R - M_T + 1)\xi_1^\star \\ &\quad + \sum_{i=2}^{M_T}(M_R - M_T + 2i - 2 + 2\alpha)\xi_i^\star \\ &\quad + \sum_{i=2}^{M_T}\zeta_i^\star + (1-2\alpha)\xi_i^\star \\ &\geq (M_R - M_T + 1)\xi_1^\star \\ &\quad + \frac{(M_T - 1)}{2}(1 + (1-2\alpha)\xi_1^\star)^+. \end{aligned} \tag{65}$$

For $\alpha \in [0, \alpha_0]$, it can be shown that the lower bound (65) is a monotonic increasing function in $\xi_1^\star$, hence $\xi_1^\star$ must attain the smallest possible value subject to the constraint $\xi_1^\star$, i.e., $\xi_1^\star = 1$, which results in

$$\begin{aligned} d &\geq d_\alpha^{(1)} \\ &\triangleq (M_R - M_T + 1) + \frac{(M_T - 1)}{2}(1 + (1-2\alpha)) \\ &= (M_R - M_T + 1)\alpha + (1-\alpha)M_R. \end{aligned} \tag{66}$$

When $\alpha \geq \alpha_0$, the lower bound in (65) is minimized by letting $1 + (1-2\alpha)\xi_1^\star = 0$. Solving for $\xi_1^\star$ yields

$$d \geq d_\alpha^{(2)} \triangleq \frac{(M_R - M_T + 1)}{2\alpha - 1}. \tag{67}$$

It is also fairly straightforward to verify that $d \geq \min\left(d_\alpha^{(1)}, d_\alpha^{(2)}\right)$ over the entire range of $\alpha \in [0, 1]$.

We proceed to (by inserting a hypothesized solution) prove that the lower bounds on the diversity order d are tight. When $\alpha \leq \alpha_0$ we consider the pair $(\boldsymbol{\xi}, \boldsymbol{\zeta})$ for which $\xi_1 = 1$, $\zeta_1 = 0$, $\xi_2 = \cdots = \xi_{M_T} = 0$, and $\zeta_2 = \cdots = \zeta_{M_T} = 1 - \alpha$. It is

straightforward to verify that $(\boldsymbol{\xi},\boldsymbol{\zeta}) \in \mathcal{O}$ and that $I(\boldsymbol{\xi},\boldsymbol{\zeta})$ equals the right-hand side of (66). Similarly, when $\alpha > \alpha_0$ the bound in (67) is achieved for $\xi_1 = (2\alpha - 1)^{-1}$, $\zeta_1 = 0$, $\xi_2 = \cdots = \xi_{M_T} = 0$, and $\zeta_2 = \cdots = \zeta_{M_T} = 0$. That $(\boldsymbol{\xi},\boldsymbol{\zeta}) \in \mathcal{O}$ for this case follows by verifying (57). This concludes the proof.

C. Eigenvector Rate Function

The purpose of this section is to establish the rate function for $\boldsymbol{\zeta}$ given in (49). Again, let $\boldsymbol{\zeta} = (\zeta_1, \ldots, \zeta_{M_T})$ be given by

$$\zeta_i = \frac{\ln \mu_i}{\ln \epsilon} \Leftrightarrow \mu_i = \epsilon^{\zeta_i}.$$

We will throughout assume that $0 < \epsilon < 1$ which implies that $\ln \epsilon < 0$ (and $\zeta_i \geq 0$ as will be seen later).

For $\mathbf{a} = (a_1, \ldots, a_{M_T})$ and $\mathbf{b} = (b_1, \ldots, b_{M_T})$ let $\mathcal{I}$ denote the *open interval* defined by

$$\mathcal{I} \in \{\boldsymbol{\zeta} \in \mathbb{R}^{M_T} \mid a_i < \zeta_i < b_i\}.$$

The goal is to first compute

$$L_{\mathcal{I}} \triangleq \lim_{\epsilon \longrightarrow \infty} \frac{\ln \Pr\{\boldsymbol{\zeta} \in \mathcal{I}\}}{\ln \epsilon} \tag{68}$$

and then extend this result to an LDP for arbitrary sets, $\mathcal{A} \subset \mathbb{R}^{M_T}$. To this end, note that $a_i < \zeta_i < b_i$ is equivalent to $\epsilon^{b_i} < \mu_i < \epsilon^{a_i}$. Further, the rotational invariance of $\mathbf{u}$ together with $\|\mathbf{u}\|^2 = 1$ implies that $\boldsymbol{\mu} \triangleq (\mu_1, \ldots, \mu_{M_T})$ (remember that $\mu_i = |u_i|^2$) is uniformly distributed over the $M_T - 1$ dimensional standard simplex [34] given by

$$\mathcal{S} \triangleq \left\{ \boldsymbol{\mu} \;\middle|\; \sum_{i=1}^{M_T} \mu_i = 1,\ \mu_i \geq 0 \right\}.$$

Since $\mu_i \leq 1$ implies that $\zeta_i \geq 0$ whenever $\epsilon < 1$ we can without loss of generality replace a_i by $a_i^+ \triangleq \max(a_i, 0)$ when computing the probability in (68). Further, $L_{\mathcal{I}} = \infty$ whenever $b_i \leq a_i^+$ for some i since $\Pr\{a_i^+ < \zeta_i < b_i\} = 0$ in this case. Finally, if $a_i > 0$ for all i it follows that

$$\sum_{i=1}^{M_T} \mu_i < \sum_{i=1}^{M_T} \epsilon^{a_i} < 1$$

for sufficiently small ϵ which implies $\Pr\{\mu_i < \epsilon^{a_i},\ \forall i\} = 0$ and $L_{\mathcal{I}} = \infty$. Thus, $L_{\mathcal{I}} < \infty$ requires that at least one $a_i \leq 0$ (or $a_i^+ = 0$). Due to the symmetry of the problem it can for the purpose of this proof be assumed that $a_{M_T}^+ = 0$.

We can thus in the following concentrate on the case where $b_i > a_i^+ \geq 0$ for $i = 1, \ldots, M_T - 1$ and $b_{M_T} > a_{M_T}^+ = 0$. Since $\mu_{M_T} = 1 - \sum_{i=1}^{M_T - 1} \mu_i$ it is convenient to parameterize the problem in terms of $(\mu_1, \ldots, \mu_{M_T - 1})$. The marginal PDF of $(\mu_1, \ldots, \mu_{M_T - 1})$ is given by

$$f(\mu_1, \ldots, \mu_{M_T - 1}) = \begin{cases} K & (\mu_1, \ldots, \mu_{M_T - 1}) \in \mathcal{P} \\ 0 & (\mu_1, \ldots, \mu_{M_T - 1}) \notin \mathcal{P} \end{cases} \tag{69}$$

where $K = (M_T - 1)! > 0$ and where

$$\mathcal{P} \triangleq \left\{ (\mu_1, \ldots, \mu_{M_T - 1}) \;\middle|\; \sum_{i=1}^{M_T - 1} \mu_i \leq 1,\ \mu_i \geq 0 \right\}.$$

That f is constant over its support follows from the uniform distribution of $\boldsymbol{\mu}$ over $\mathcal{S}$. Thus,

$$\Pr\{\boldsymbol{\zeta} \in \mathcal{I}\} = K \mathrm{vol}[\mathcal{C} \cap \mathcal{P}] \tag{70}$$

where

$$\mathcal{C} \triangleq \{(\mu_1, \ldots, \mu_{M_T - 1}) | \epsilon^{b_i} \leq \mu_i \leq \epsilon^{a_i^+},\ i = 1, \ldots, M_T\}.$$

and where $\mu_{M_T} = 1 - \sum_{i=1}^{M_T - 1} \mu_i$. By (70) it follows that

$$\Pr\{\boldsymbol{\zeta} \in \mathcal{I}\} \leq K \mathrm{vol}[\mathcal{C}] \leq K \prod_{i=1}^{M_T - 1} \epsilon^{a_i^+} = K \epsilon^{\sum_{i=1}^{M_T - 1} a_i^+}$$

and

$$\liminf_{\epsilon \longrightarrow \infty} \frac{\ln \Pr\{\boldsymbol{\zeta} \in \mathcal{I}\}}{\ln \epsilon} \geq \sum_{i=1}^{M_T - 1} a_i^+ = \sum_{i=1}^{M_T} a_i^+$$

where the last equality follows since $a_{M_T}^+ = 0$ by assumption.

In order to provide a lower bound on $\Pr\{\boldsymbol{\zeta} \in \mathcal{I}\}$ consider the open interval

$$\mathcal{B} \triangleq (c_1 \epsilon^{a_1^+}, c_2 \epsilon^{a_1^+}) \times \cdots \times (c_1 \epsilon^{a_{M_T - 1}^+}, c_2 \epsilon^{a_{M_T - 1}^+})$$

for some constants $c_1 < c_2 \leq {M_T}^{-1}$. We aim to show that $\mathcal{B} \subset \mathcal{C} \cap \mathcal{P}$ for small $\epsilon > 0$. Since

$$\sum_{i=1}^{M_T - 1} c_2 \epsilon^{a_1^+} \leq (M_T - 1) c_2 \leq 1$$

and since $c_1 \epsilon^{a_1^+} > 0$ for $i = 1, \ldots, M_T - 1$ it follows that $\mathcal{B} \subset \mathcal{P}$. What remains to be shown is that $\mathcal{B} \subset \mathcal{C}$. To this end, note that for sufficiently small ϵ it follows that $\epsilon^{b_i} \leq c_1 \epsilon^{a_i}$ for $i = 1, \ldots, M_T - 1$ since $b_i > a_i^+$. Also,

$$\begin{aligned} \mu_{M_T} &= 1 - \sum_{i=1}^{M_T - 1} \mu_i \geq 1 - \sum_{i=1}^{M_T - 1} c_2 \epsilon^{a_i^+} \\ &\geq 1 - c_2 (M_T - 1) \geq \frac{1}{M_T} \geq \epsilon^{b_{M_T}} \end{aligned}$$

for sufficiently small ϵ. Finally, since $a_{M_T}^+ = 0$ by assumption $\mu_{M_T} \leq \epsilon^{a_{M_T}^+}$ is trivially satisfied. Thus, again for small ϵ, it follows that $\mathcal{B} \subset \mathcal{C}$ which together with $\mathcal{B} \subset \mathcal{P}$ implies $\mathcal{B} \subset \mathcal{C} \cap \mathcal{P}$ as previously asserted. However, since

$$\mathrm{vol}[\mathcal{B}] = (c_2 - c_1)^{M_T - 1} \prod_{i=1}^{M_T - 1} \epsilon^{a_i^+}$$

and since $(c_2 - c_1)^{M_T - 1} > 0$ it follows that

$$\limsup_{\epsilon \longrightarrow \infty} \frac{\ln \Pr\{\boldsymbol{\zeta} \in \mathcal{I}\}}{\ln \epsilon} \leq \limsup_{\epsilon \longrightarrow \infty} \frac{\ln \mathrm{vol}[\mathcal{B}]}{\ln \epsilon} \leq \sum_{i=1}^{M_T - 1} a_i^+ = \sum_{i=1}^{M_T} a_i^+.$$

So far, it has been shown that

$$L_{\mathcal{I}} \triangleq \lim_{\epsilon \longrightarrow \infty} \frac{\ln \Pr\{\boldsymbol{\zeta} \in \mathcal{I}\}}{\ln \epsilon} = \sum_{i=1}^{M_T} a_i^+. \tag{71}$$

if $a_i^+ = 0$ for some i and $b_i > a_i^+$ for all i and that $L_{\mathcal{I}} = \infty$ otherwise.

By appealing to [16, Theorem 4.1.11], it now follows that $\boldsymbol{\zeta}$ satisfies (46) for *compact* sets $\mathcal{A} \subset \mathbb{R}^{M_T}$ with a rate function

$$I_{\zeta}(\boldsymbol{\zeta}) = \sup_{\{\mathcal{I}: \boldsymbol{\zeta} \in \mathcal{I}\}} L_{\mathcal{I}} \tag{72}$$

where the supremum is taken over all open intervals containing $\boldsymbol{\zeta}$. To verify that (72) coincides with (49) note that if $\zeta_i < 0$ for some i then by selecting $\zeta_i < b_i < 0$ it follows that the supremum in (72) is ∞. Similarly, if $\zeta_i > 0$ for $i = 1, \ldots, n$ the same thing follows by selecting $\zeta_i > a_i > 0$ for $i = 1, \ldots, i$. Therefore, $I_{\zeta}(\boldsymbol{\zeta}) = \infty$ unless $\zeta_1, \ldots, \zeta_{M_T} \geq 0$ with equality for some ζ_i. In that case that $I_{\zeta}(\boldsymbol{\zeta}) < \infty$ is equal to (49) since $\boldsymbol{\zeta} \in \mathcal{I}$ requires $a_i < \zeta_i < b_i$ for $i = 1, \ldots, M_T$. By additionally verifying that $\boldsymbol{\zeta}$ is *exponentially tight* [16] it follows that (46) is satisfied for all sets $\mathcal{A} \subset \mathbb{R}^{M_T}$ with this rate function.

ACKNOWLEDGMENT

The authors would like to thank G. Reise for providing the C code for the sphere decoder variant.

REFERENCES

[1] A. Paulraj, R. U. Nabar, and D. Gore, *Introduction to Space-Time Wireless Communications*. Cambridge, U.K.: Cambridge Univ. Press, 2003.

[2] E. Agrell, T. Eriksson, A. Vardy, and K. Zeger, "Closest point search in lattices," *IEEE Trans. Inf. Theory*, vol. 48, no. 8, pp. 2201–2214, Aug. 2002.

[3] M. Damen, A. Chkeif, and J. Belfiore, "Lattice code decoder for space-time codes," *IEEE Comm. Lett.*, vol. 4, no. 5, pp. 161–163, May 2000.

[4] J. Jaldén and B. Ottersten, "On the complexity of sphere decoding in digital communications," *IEEE Trans. Signal Process.*, vol. 53, pp. 1474–1484, Apr. 2005.

[5] J. Jaldén and B. Ottersten, "On the limits of sphere decoding," in *Proc. IEEE Int. Symp. Inf. Theory (ISIT)*, Sep. 2005, pp. 1691–1695.

[6] G. D. Golden, G. J. Foschini, R. A. Valenzuela, and P. W. Wolniansky, "Detection algorithm and initial laboratory results using V-BLAST space-time communications architecture," *Elect. Lett.*, vol. 35, pp. 14–16, Jan. 1999.

[7] W.-J. Choi, R. Negi, and J. M. Cioffi, "Combined ML and DFE decoding for the V-BLAST system," in *Proc. IEEE ICC-00*, New Orleans, LA, Jun. 2000, pp. 18–22.

[8] S. Moshavi, "Multi-user detection for DS-CDMA communications," *IEEE Comm. Mag.*, vol. 34, no. 10, pp. 124–136, Oct. 1996.

[9] H. Artés, D. Seethaler, and F. Hlawatsch, "Efficient detection algorithms for MIMO channels: A geometrical approach to approximate ML detection," *IEEE Trans. Signal Process.*, vol. 51, pp. 2808–2820, Nov. 2003.

[10] J. Maurer, G. Matz, and D. Seethaler, "Low-complexity and full-diversity MIMO detection based on condition number thresholding," in *Proc. IEEE ICASSP'07*, Honolulu, HI, Apr. 2007, pp. 61–64.

[11] A. K. Lenstra, H. W. Lenstra, Jr, and L. Lovász, "Factoring polynomials with rational coefficients," *Math. Ann.*, vol. 261, pp. 515–534, 1982.

[12] M. Taherzadeh, A. Mobasher, and A. Khandani, "LLL lattice-basis reduction achieves the maximum diversity in MIMO systems," in *Proc. IEEE ISIT 2005*, Adelaide, Australia, Sep. 2005, pp. 1300–1304.

[13] J. Jaldén, L. G. Barbero, B. Ottersten, and J. S. Thompson, "Full diversity detection in MIMO systems with a fixed-complexity sphere decoder," in *Proc. IEEE ICASSP'07*, Honolulu, HI, Apr. 2007, vol. 3, pp. 49–52.

[14] J. Jaldén, L. G. Barbero, B. Ottersten, and J. S. Thompson, "The error probability of the fixed-complexity sphere decoder," *IEEE Trans. Signal Process.*, vol. 57, no. 7, pp. 2711–2720, Jul. 2009.

[15] M. Stojnic, H. Vikalo, and B. Hassibi, "Speeding up the sphere decoder with H-infinity and SDP inspired lower bounds," *IEEE Trans. Signal Process.*, vol. 56, pp. 712–726, Feb. 2008.

[16] A. Dembo and O. Zeitouni, *Large Deviations Techniques and Applications*, 2nd ed. New York: Springer-Verlag, 1998.

[17] R. A. Horn and C. R. Johnson, *Matrix Analysis*. Cambridge, U.K.: Cambridge Univ. Press, 1999.

[18] E. Biglieri, G. Taricco, and A. Tulino, "Performance of space-time codes for a large number of antennas," *IEEE Trans. Inf. Theory*, vol. 48, no. 9, pp. 1794–1803, Jul. 2002.

[19] D. A. Gore, J. Robert, W. Heath, and A. J. Paulraj, "Transmit selection in spatial multiplexing systems," *IEEE Comm. Lett.*, vol. 6, no. 11, pp. 491–493, Nov. 2002.

[20] M. Varanasi, "Group detection for synchronous Gaussian code-division multiple-access channels," *IEEE Trans. Inf. Theory*, vol. 41, no. 4, pp. 1083–1096, Jul. 1995.

[21] G. H. Golub and C. F. Van Loan, *Matrix Computations*, 3rd ed. Baltimore, MD: Johns Hopkins Univ. Press, 1996.

[22] B. Hassibi and H. Vikalo, "On the sphere-decoding algorithm I. Expected complexity," *IEEE Trans. Signal Process.*, vol. 53, no. 8, pp. 2806–2812, Aug. 2005.

[23] M. Damen, H. E. Gamal, and G. Caire, "On maximum-likelihood detection and the search for the closest lattice point," *IEEE Trans. Inf. Theory*, vol. 49, no. 10, pp. 2389–2402, Oct. 2003.

[24] A. D. Murugan, H. E. Gamal, M. O. Damen, and G. Caire, "A unified framework for tree search decoding: Rediscovering the sequential decoder," *IEEE Trans. Inf. Theory*, vol. 52, no. 3, pp. 933–953, Mar. 2006.

[25] A. Burg, M. Borgmann, M. Wenk, M. Zellweger, W. Fichtner, and H. Bölcskei, "VLSI implementation of MIMO detection using the sphere decoding algorithm," *IEEE J. Solid-State Circuits*, vol. 40, no. 7, pp. 1566–1577, Jul. 2005.

[26] C. P. Schnorr and M. Euchner, "Lattice basis reduction: Improved practical algorithms and solving subset sum problems," *Math. Programming*, vol. 66, no. 1–3, pp. 181–199, Aug. 1994.

[27] M. O. Damen, H. E. Gamal, and G. Caire, "MMSE-GDFE lattice decoding for under-determined linear channels," in *Proc. Conf. Inf. Sci. Syst.*, Princeton, NJ, Mar. 2004.

[28] G. E. Forsythe and P. Henrici, "The cyclic Jacobi method for computing the principal values of a complex matrix," *Trans. Amer. Math. Soc.*, vol. 94, pp. 1–23, 1960.

[29] J. Jaldén and G. Matz, "MIMO receiver diversity in general fading," in *Proc. IEEE ICASSP'08*, Las Vegas, NV, Apr. 2008, pp. 2837–2840.

[30] Z. Wang and G. B. Giannakis, "A simple and general parameterization quantifying performance in fading channels," *IEEE Trans. Commun.*, vol. 51, no. 8, pp. 1389–1398, Aug. 2003.

[31] D. Tse and P. Viswanath, *Fundamentals of Wireless Communication*. Cambridge, U.K.: Cambridge Univ. Press, 2005.

[32] L. Zheng and D. Tse, "Diversity and multiplexing: A fundamental tradeoff in multiple antenna channels," *IEEE Trans. Inf. Theory*, vol. 49, no. 5, pp. 1073–1096, May 2003.

[33] A. Tulino and S. Verdú, "Random matrix theory and wireless communications," *Foundations and Trends in Commun. and Inf. Theory*, vol. 1, no. 1, 2004.

[34] S. S. Wilks, *Mathematical Statistics*. New York: Wiley, 1962.

[35] J. Maurer, G. Matz, and D. Seethaler, "On the diversity-complexity tradeoff in MIMO spatial multiplexing systems," in *Proc. Asilomar Conf. Signals, Syst., Comput.*, Pacific Grove, CA, Oct.-Nov. 2006, pp. 2077–2081.

[36] K. Lee and J. Chun, "ML symbol detection based on the shortest path algorithm for MIMO systems," *IEEE Trans. Signal Process.*, vol. 55, pp. 5477–5484, Nov. 2007.

Johannes Maurer (M'09) received the Dipl.-Ing. and Dr.techn. degrees in electrical/communication engineering from the Vienna University of Technology, Vienna, Austria, in 2005 and 2009, respectively.

From 2005 to 2009, he was a Research and Teaching Assistant at the Institute of Communications and Radio Frequency Engineering, Vienna University of Technology. His research interests are in wireless communications with emphasis on MIMO multi-user signal processing.

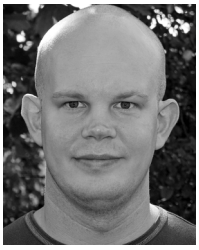

Joakim Jaldén (M'08) received the M.Sc. and Ph.D. degrees in electrical engineering from the Royal Institute of Technology (KTH), Stockholm, Sweden, in 2007 and 2002, respectively.

From July 2007 to June 2009, he held a postdoctoral research position at the Vienna University of Technology, Vienna, Austria. He also studied at Stanford University, Stanford, CA, from September 2000 to May 2002, and worked at ETH, Zürich, Switzerland, as a Visiting Researcher, from August to September, 2008. In July 2009, he joined the Signal Processing Lab within the School of Electrical Engineering at KTH, as an Assistant Professor.

Dr. Jaldén has been awarded the IEEE Signal Processing (SP) Society's 2006 Young Author Best Paper Award and the first prize in the Student Paper Contest at the 2007 International Conference on Acoustics, Speech and Signal Processing (ICASSP) for his work on MIMO communications. He is also a recipient of the Ingvar Carlsson Award issued in 2009 by the Swedish Foundation for Strategic Research, and the grant, "Honor Graduate Student Position," awarded in 2002 by the dean's office at KTH.

Dominik Seethaler (M'06) received the Dipl.-Ing. and Dr.techn. degrees in electrical/communication engineering from Vienna University of Technology, Vienna, Austria, in 2002 and 2006, respectively.

From 2002 to 2007, he was a Research and Teaching Assistant at the Institute of Communications and Radio-Frequency Engineering, Vienna University of Technology. Since September 2007, he has been a Postdoctoral Researcher at the Communication Technology Laboratory, ETH Zurich, Zurich, Switzerland. His research interests are in wireless communications with emphasis on MIMO multi-user signal processing.

Gerald Matz (S'95–M'01–SM'07) received the Dipl.-Ing. and Dr.techn. degrees in electrical engineering and the habilitation degree for communication systems, all from Vienna University of Technology, Vienna, Austria, in 1994, 2000, and 2004, respectively.

Since 1995, he has been with the Institute of Communications and Radio-Frequency Engineering, Vienna University of Technology, where he currently holds a tenured position as Associate Professor. From March 2004 to February 2005, he was on leave as an Erwin Schrödinger Fellow with the Laboratoire des Signaux et Systèmes, L'École Supérieure d'Électricité, Gif-sur-Yvette, France. During Summer 2007, he was a Guest Researcher with the Communication Theory Lab at ETH Zurich, Switzerland. He has directed or actively participated in several research projects funded by the Austrian Science Fund (FWF) and by the European Union. He has published some 120 papers in international journals, conference proceedings, and edited books. His research interests include wireless communications, statistical signal processing, and information theory.

Prof. Matz serves as a member of the IEEE Signal Processing Society Technical Committee on Signal Processing for Communications and Networking and as Associate Editor for the IEEE TRANSACTIONS ON SIGNAL PROCESSING and for the EURASIP journal *Signal Processing*. From 2004 to 2008, he was an Associate Editor for the IEEE SIGNAL PROCESSING LETTERS. He was Technical Program Co-Chair of EUSIPCO 2004 and has been member of the Program Committee of numerous international conferences. In 2006, he received the Kardinal Innitzer Most Promising Young Investigator Award.